SA(IR)-160

UNITED STATES DEPARTMENT OF THE INTERIOR
GEOLOGICAL SURVEY

SAUDI ARABIAN PROJECT REPORT 160

TUNGSTEN ANOMALIES IN THE UYAIJAH RING STRUCTURE

KUSHAYMIYAH IGNEOUS COMPLEX
KINGDOM OF SAUDI ARABIA

SECTION A-GEOLOGY AND GEOCHEMISTRY
OF THE UYAIJAH RING STRUCTURE
By Paul K. Theobald and Glenn H. Allcott

SECTION B-REGIONAL GEOPHYSICS
By Vincent J. Flanigan and Gordon E. Andreasen

This report is preliminary and has not been edited or reviewed for conformity with U.S. Geological Survey standards and nomenclature. These data are preliminary and should not be quoted without permission.

PREPARED FOR
DIRECTORATE GENERAL OF MINERAL RESOURCES
MINISTRY OF PETROLEUM AND MINERAL RESOURCES
JIDDAH, SAUDI ARABIA

1977

CONTENTS

	Page
ABSTRACT	1
SECTION A - GEOLOGY AND GEOCHEMISTRY OF THE UYAIJAH RING STRUCTURE by Paul K. Theobald and Glenn H. Allcott	1A
INTRODUCTION	2
SELECTION OF THE UYAIJAH RING STRUCTURE	5
General geology	5
Geophysical data	7
Geochemical orientation survey	9
GEOLOGY OF THE UYAIJAH RING STRUCTURE	15
Lithologic units	17
Murdama Group	17
Calc-alkaline igneous rocks	19
Diorite, granodiorite, and gabbro	19
Porphyritic granodiorite	20
Quartz monzonite and aplite	22
Alkaline granite suite	24
Quartz veins and alteration	26
Late dike rocks	28
Structure	29
Summary of geologic history	32
GEOCHEMISTRY OF THE UYAIJAH RING STRUCTURE	33
General features	33
The anomalies	56
SUMMARY AND RECOMMENDATION	63
LITERATURE CITED	65

CONTENTS (Cont'd).

Page

SECTION B - REGIONAL GEOPHYSICS by Vincent J. Flanigan and and Gordon E. Andreasen..... 67

INTRODUCTION..... 68

GAMMA RADIATION..... 68

Survey instrumentation and procedures..... 73

Data reduction..... 73

Area 1..... 74

Area 2..... 76

Area 3..... 77

Area 4..... 78

AREOMAGNETIC INTERPRETATION..... 79

CONCLUSIONS..... 85

LITERATURE CITED..... 86

ILLUSTRATIONS

Plate 1. Geographic and physiographic map of the Uyaijah ring structure showing the location of samples and areas recommended for further work. .....Back pocket

2. Geology of the ring structure near Al Uyaijah, Kingdom of Saudi Arabia.....Back pocket

Figure 1. Index map of western Saudi Arabia showing the location of the Kushaymiyah area and the Uyaijah ring structure..... 3

2. Histograms of the barium, boron, and nickel content of surficial debris as a function of the size fraction.....11

ILLUSTRATIONS (Contd.)

Page

Figure 3. Diagram showing composition of six rock samples from the Uyaijah ring structure..... 14
4. Cumulative frequency vs log ppm tungsten for samples from location 60041..... 38
5. Distribution of copper, Uyaijah ring structure..... 42
6. Distribution of nickel, Uyaijah ring structure..... 42
7. Distribution of magnesium, Uyaijah ring structure.. 43
8. Distribution of vanadium, Uyaijah ring structure... 43
9. Distribution of calcium, Uyaijah ring structure.... 44
10. Distribution of manganese, Uyaijah ring structure.. 44
11. Distribution of chromium, Uyaijah ring structure... 45
12. Distribution of scandium, Uyaijah ring structure... 45
13. Distribution of cobalt, Uyaijah ring structure..... 46
14. Distribution of iron, Uyaijah ring structure..... 46
15. Distribution of yttrium, Uyaijah ring structure.... 47
16. Distribution of titanium, Uyaijah ring structure... 47
17. Distribution of boron, Uyaijah ring structure..... 48
18. Distribution of barium, Uyaijah ring structure..... 48
19. Distribution of zirconium, Uyaijah ring structure.. 49
20. Granodiorite index map, Uyaijah ring structure..... 49
21. Factors resulting from successive rotations of the 16 variable matrix..... 52
22. Plot of variation of magnetic character vs relative concentration of 19 elements in the heavy-mineral suite of sample location 60041..... 54

ILLUSTRATIONS (Cont'd.)

Page

Figure 23. Tungsten and molybdenum content of heavy-mineral concentrates from the Uyaijah ring structure..... 54

24. Map of the Uyaijah area showing the location of anomalous tungsten, lanthanum, molybdenum, and bismuth..... 57

25. Selected structural elements of the Uyaijah ring structure in relation to anomalous concentrations of tungsten in heavy-mineral concentrates..... 59

26. Generalized geologic map of the Kushaymiyah area showing isoradiometric contours (total count)..... 69

27. Generalized geologic map of the Kushaymiyah area showing isoradiometric contours (uranium)..... 70

28. Generalized geologic map of the Kushaymiyah area showing isoradiometric contours (thorium)..... 71

29. Generalized geologic map of the Kushaymiyah area showing isoradiometric contours (potassium)..... 72

30. Total intensity aeromagnetic map of the Kushaymiyah area..... 80

31. Generalized geologic map of the Kushaymiyah area showing major magnetic features..... 81

32. Observed and theoretical total intensity magnetic profiles across the Uyaijah ring structure..... 84

TABLES

Page

Table 1. Precision and accuracy of 6-step semiquantitative analysis based on replicate analyses of standard rocks G-1, G-2, and GSP-1.....36 & 37

2. Range, mean, and standard deviation of 21 elements based on analyses of 22 samples from sample loca-60041.....41

SECTION A

GEOLOGY AND GEOCHEMISTRY OF THE UYAIJAH RING STRUCTURE

by

Paul K. Theobald and Glenn H. Allcott

TUNGSTEN ANOMALIES IN THE UYAIJAH RING STRUCTURE KUSHAYMIYAH IGNEOUS COMPLEX KINGDOM OF SAUDI ARABIA

SECTION A
GEOLOGY AND GEOCHEMISTRY OF THE UYAIJAH RING STRUCTURE

by

Paul K. Theobald and Glenn H. Allcott

SECTION B
REGIONAL GEOPHYSICS

by

Vincent J. Flanigan and Gordon E. Andreasen

U. S. Geological Survey

ABSTRACT

Anomalous amounts of tungsten, molybdenum, and bismuth are present in the Uyaijah ring structure of the Kushaymiyah igneous complex in the eastern part of the Precambrian shield of the Kingdom of Saudi Arabia. The complex includes four major rock units, the Murdama Group, porphyritic granodiorite, quartz monzonite, alkaline granite, and areas enriched in silica. Structural and compositional relationships among some of the rock units are defined in part by aeromagnetic and gamma-ray spectrometric geophysical data. Geochemical data from -10 +30 mesh surficial debris were primarily related to the composition of the major rock units, whereas data from heavy-mineral concentrates were used to establish the location of tungsten-molybdenum-bismuth anomalies.

Two areas of about 40 sq km each are occupied by tungsten-molybdenum-bismuth anomalies interpreted to be related to the alkaline granite. One of these is a contact metasomatic anomaly; the other is related to leakage from an inferred underlying cupola of the alkaline granite. These two anomalous areas are recommended for further investigatio

INTRODUCTION

Tungsten and molybdenum anomalies in the vicinity of Al Kushaymiyah in the eastern part of the 1:500,000-scale Southern Najd quadrangle (Jackson and others, 1963) have attracted sporadic attention since they were first described by Whitlow (1966a, 1966b, 1971). Re-emphasis of the potential of these anomalies (Theobald, 1971) led to the present work, which proposes that the original relatively large area of 1000 sq km or more be reduced to two areas of about 40 sq km each -- a reasonable size for geologic exploration. The greater part of this report describes the geologic parameters used to identify the two smaller areas. Recommendations for continued work are proposed.

Al Kushaymiyah (fig. 1) is about 200 km south of Ad Dawadami in an area where scattered nafuds (sand seas) occupy a physiographic pattern controlled largely by petrographic and structural features of the bedrock. Terrane underlain by granitic rocks and, in particular, by the Uyaijah ring structure within the Kushaymiyah complex is of principal geologic interest. The granitic terrane is generally subdued pediment areas from which rounded inselbergs rise. The prominent massifs of Jabals Al Hawshah and Hawshat Ibn Huwayl, developed on large masses of alkaline granite, are an exception to the relatively subdued topography of the granitic rock outcrop areas and identify the alkaline granite as the more resistant of the granitic suite. Similar relations can be seen in the Kushaymiyah complex where the most prominent inselbergs, Jabals Buhairan and Abu Khurg, are developed on the alkaline granites.

The Kushaymiyah complex exhibits a regional change in level and physiographic expression, becoming generally more subdued and lower

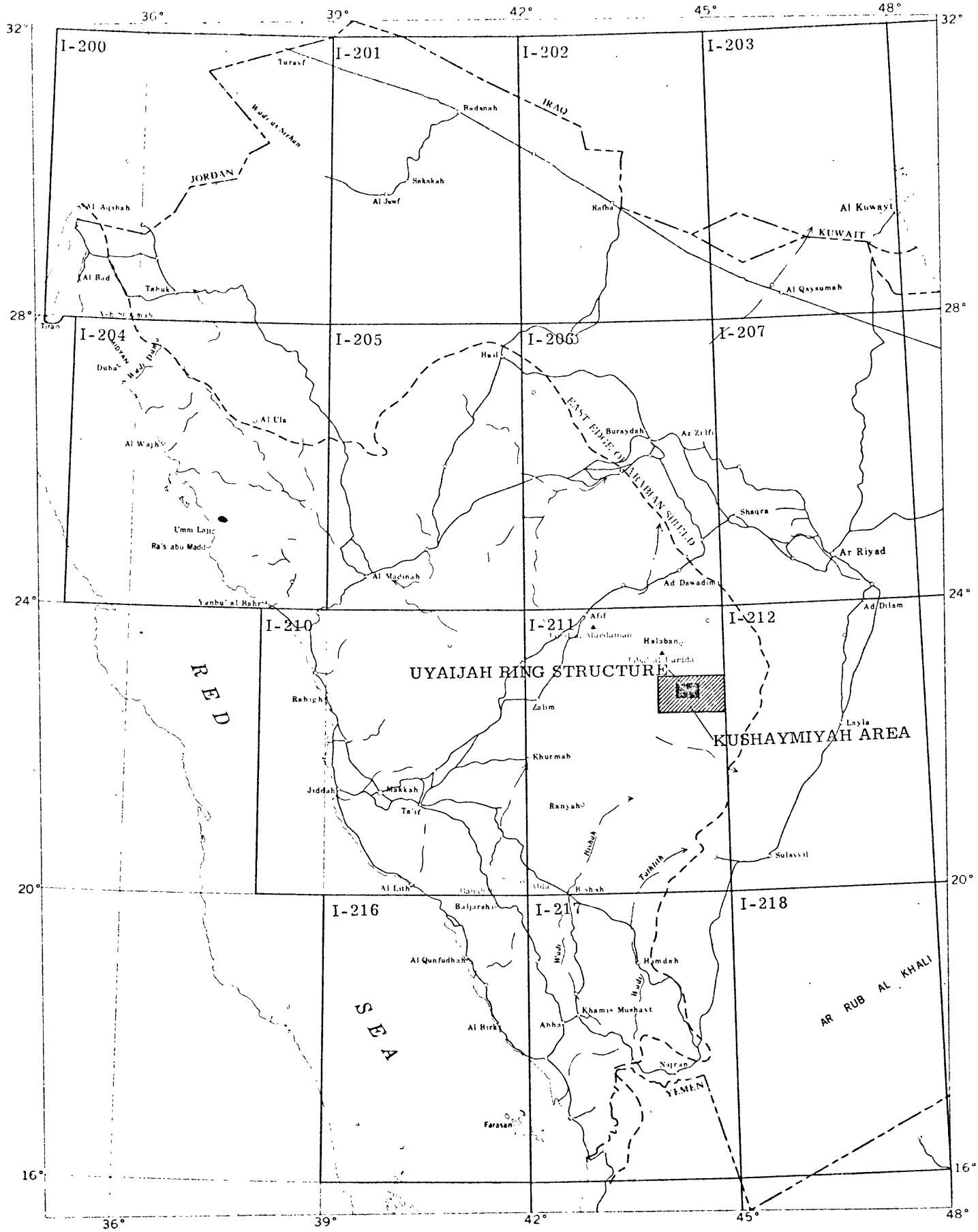

Figure 1.- Index map of western Saudi Arabia showing the location of the Kushaymiyah area and the Uyaijah ring structure.

to the northeast toward the Nafud as Sirrah. In the Uyaijah ring of the complex the northeasterly change is stepwise. Because these topographic changes may affect the composition of samples obtained from surficial debris, the most prominent of the steps have been superimposed on the sample net (plate 1). The effect of these steps on the composition of the samples is crucial to later discussions of the geochemistry in the area covered by plate 1. The steps are most commonly marked by a stable dune front which makes a steep sloping face of aeolian sand. Samples collected on or in front of the steps generally contain more aeolian sand than samples taken at a distance from the steps.

The prominent, west-northwest-trending step extending across most of the ring is structurally controlled. It separates the southern third of the ring, with southerly drainage, from the northern two-thirds of the ring which drains generally northward. The drainage divide at this step has apparently migrated 1 to 2 km to the south from the controlling structure, which is the transverse fault zone.

The size of the exploration target was narrowed to the two areas of the Uyaijah ring structure shown on plate 1 through the combined efforts of several people and organizations. For Section A of this report, the original work of Whitlow, who made available his field notes and additional interpretations of them in light of more recent data, provided the base for the recognition of the general target. Unpublished manuscripts and maps of Al Kushaymiyah and Jabal Al Hawshah quadrangles, (Lancombe and Letalenet, 1970), prepared by the French Bureau de Recherches Géologiques et Minières (BRGM), give the regional geologic setting and are reproduced here with the permission of

Dr. J. J. Altmann, Chief of BRGM in Jiddah. Messieurs Delfour and Letalenet of BRGM have been especially helpful in discussions of the regional geologic relations. Mohammed Jambi made spectrographic analyses of heavy-mineral concentrates, A. A. Redhwi and I. N. Nagvi did colorimetric analyses, and E. Brady and Mustafa Mawad analyzed samples of wadi sediment.

SELECTION OF THE UYAIJAH RING STRUCTURE

The original proposal of Al Kushaymiyah as a target for a Colorado-type molybdenite deposit (Theobald, 1971) was known to encompass too large an area for any reasonable scale of exploration, but that proposal visualized an areal study to reduce Al Kushaymiyah to more specific targets for detailed examination. The work reported here succeeded in that objective, owing to the use made of the geologic maps by the BRGM, the interpretation of aeromagnetic data by Andrew Griscom, and the gamma-ray spectrometry by Vincent Flanigan. These data permitted fairly narrow geographic focusing of the field work. Information from these sources coupled with that derived from about 1 week of geochemical orientation in the field allowed identification of the Uyaijah ring structure as the most promising target area.

General geology

The tin anomalies and the tungsten and molybdenum highs identified by Whitlow (1966a; 1966b) are associated in large part with a pair of alkalic granite masses at Jabal Al Hawshah and at Jabal Hawshat Ibn Huwayl in the Jabal Al Hawshsh quadrangle. Both masses are uniformly rich in a suite of elements that includes rare earths, beryllium, lead, and tin. Samples from the northern mass are commonly rich in niobium, and tungsten or molybdenum may also be enriched. The assemblage of

elements, and their rather uniformly high but not spectacular levels of concentration, is here interpreted to mean that these elements do not constitute immediate targets for ore deposits of the type we have anticipated. More detailed petrochemical studies of these masses of alkalic granite would yield valuable information on this unusual suite of rocks and could possibly lead to discovery of vein, segregation, or contact deposits. The Jabal Al Hawshah and Jabal Hawshat Ibn Huwayl masses, however, are assigned a relatively low priority for exploration.

The Jabal Fahwah pluton of calc-alkaline granite, also in the Jabal Al Hawshah quadrangle, is uniformly rich in titanium, vanadium, and molybdenum relative to the other granitic rocks of the area. The high molybdenum may reflect an environment rich in this element and possibly to economic concentrations of the metal. Like its alkaline neighbors, this pluton has considerable petrochemical interest but must, from the limited objectives of this study, be assigned a low priority for exploration.

A third area that has a low exploration priority is southwest of the Najd fault in the western part of Al Kushaymiyah quadrangle. Here, detailed mapping by BRGM has reclassified a series of rocks, originally assigned to the calc-alkaline granitic suite, as being gneiss and migmatite of probable Halaban age; that is, pre- rather than post-Murdama in age. Moderate geochemical highs in molybdenum, tungsten, or tin from reconnaissance work in this area (Whitlow, 1966b) may be assigned with fair confidence to pegmatites identified by BRGM. These pegmatites have been rejected by the BRGM as of little economic significance, a conclusion with which we concur. A single sample

rich in tungsten and molybdenum and having 300 ppm tin was obtained by Whitlow along the east edge of the Nafud Al Hawrizah near a locality where BRGM later obtained a sample rich in copper. Pegmatites are not known in this area, and the copper sample is clearly not derived from the type of deposit being sought in this investigation. Although the copper occurrence, has been given no further attention here, it remains to be explained.

The complex Al Kushaymiyah mass is the prime target area. The BRGM mapping shows Al Kushaymiyah to be a multilobed mass of calc-alkaline granitic rocks suggestive of overlapping cupolas at the top of a major intrusive. Several of the lobes are further defined within the mass by arcuate dikes of alkaline granite. Al Uyaijah lobe is particularly well defined. Interestingly, most of Whitlow's tungsten-rich sediment samples came from this lobe, but some came from the vicinity of the small lobe east of Al Uyaijah lobe. He collected few samples west of Al Uyaijah. The entire Al Kushaymiyah complex is transected by the shear zone of the Najd trend along wnich Whitlow described alteration.

Geophysical data

Aeromagnetic data were available and were being interpreted at the time this investigation was begun. Airborne gamma-ray spectrometric data covering the area also were being reduced. Both of these studies support the recommendations advanced in this report.

The aeromagnetic data, as interpreted by Griscom, defines two major fault zones that subdivide the Kushaymiyah area into three parts (see Section B). The Najd fault separates the linear anomalies over Halaban rocks in the southwestern part of the Kushaymiyah quadrangle

from the more subdued magnetic relief over Murdama rocks to the northeast. A north-northwest-trending fault extends from near the center of the south boundary of the Jabal Al Hawshaw quadrangle into the northeast corner of Al Kushaymiyah quadrangle, separating the well-defined residual anomalies over the Jabal Fahwah and Al Kushaymiyah granitic complex from the low amplitude magnetic pattern over the calc-alkaline and alkaline granitic masses to the east. A third, rather ill-defined fault but of interest to this discussion parallels the Najd fault and traverses the Kushaymiyah complex axially. This fault apparently terminates against the north-northeast-trending fault to the east.

The Jabal Fahwah and Al Kushaymiyah complexes are clearly defined by remnant magnetic anomalies. The Kushaymiyah complex in particular appears as a cluster of overlapping, nearly circular magnetic bodies, many of which have a shell-like, double border. There is a suggestion of additional shallow granitic material south of the west end of the complex, and a similar suggestion of a shallow connecting granitic mass between the Kushaymiyah complex and the two calc-alkaline granite bodies at the northwest boundary of the Kushaymiyah quadrangle. The Uyaijah ring is the best defined and most complete of the magnetic structures. This is here interpreted to mean that it is the youngest. The magnetic features of the Uyaijah ring are, however, somewhat confused where the central fault crosses the west edge of the ring. North of the fault the Uyaijah ring appears to be nearly complete. South of the fault more evidence is seen for continuity of the adjacent, magnetically reversed ring than for continuity of the Uyaijah ring. Along the east boundary of the Uyaijah ring evidence is again present

for discontinuity in the rather featureless magnetic area corresponding to a small local calc-alkaline mass. The Jabal Fahwah pluton is a well defined magnetic structure, the anomaly of which, at the south end, has the greatest magnetic amplitude of any anomaly on the mosaic. A small magnetic anomaly west of Jabal Fahwah and south of Al Uyaijah defines a small calc-alkaline pluton.

The results of gamma-ray spectrometry are described in more detail in Section B. For the purpose of the immediate discussion it is adequate to note the high radiation levels over the two alkaline granites of the Jabal Al Hawshah quadrangle, the generally low radiation level over the Jabal Fahwah pluton, and the clear definition of the radioactive Uyaijah ring within the Kushaymiyah complex. These features serve to confirm the conclusions already presented: (1) the Hawshah alkaline granites are unusual granites, (2) the Fahwah pluton is a more mafic body, and (3) the Uyaijah ring of the Kushaymiyah complex is the most promising target for deposits of tungsten and molybdenum.

Geochemical orientation survey

Four preliminary geochemical orientation traverses were laid out to cover the Kushaymiyah complex and the small pluton to the south. The primary orientation traverse trends N.25°E. across the Uyaijah ring structure and corresponds approximately to flight line 16, area I, of the airborne radiation survey. Two samples weighing about 10 kg each were collected on 1 km intervals at each of 25 sites along the traverse, and continuous geologic notes were taken. A second traverse extends S.87°W. from near the center of the Uyaijah ring to the west edge of the Kushaymiyah complex. Single samples weighing

10 kg were collected at 2 km intervals along 28 km of traverse. This traverse indicates that cores of the rings to the west of Al Uyaijah are of more mafic nature. The third traverse extends S.73°E. from the center of the Uyaijah ring. Samples weighing 10 kgs were taken on 1 km spacing for 15 km across the eastern part of the Uyaijah ring structure and the small calc-alkaline mass to the east. On the fourth traverse, 8 samples were collected at 1 km spacing along a line oriented N.57°W. to cover the small calc-alkaline mass south of the Uyaijah ring. The sample at each locality was made from surficial debris, either wadi sediment or pediment cover, because this material offered the only reasonable source of an averaged sample in the area of representation necessarily assigned each sample.

One each of the samples taken at the 25 localities on the primary orientation traverse was sieved to five size fractions and each fraction was analysed spectrographically for 23 elements. Heavy-mineral concentrates were panned from the other samples on the primary traverse. After removal of ferromagnetic material, the concentrates were colorimetrically analysed for tungsten and molybdenum.

The 14 trace elements consistently detected spectrographically in the sieved samples show consistent distribution patterns. Three elements, barium, boron, and nickel, have been chosen to illustrate this pattern and to demonstrate why the results of the orientation survey led to the choice of the -10 +30 mesh fraction for subsequent sampling (fig. 2). The results of the analyses of the -200 mesh fractions of all 25 samples for the 14 consistently present elements show clearly that measurable natural variation is lacking in the -200 mesh fractions.

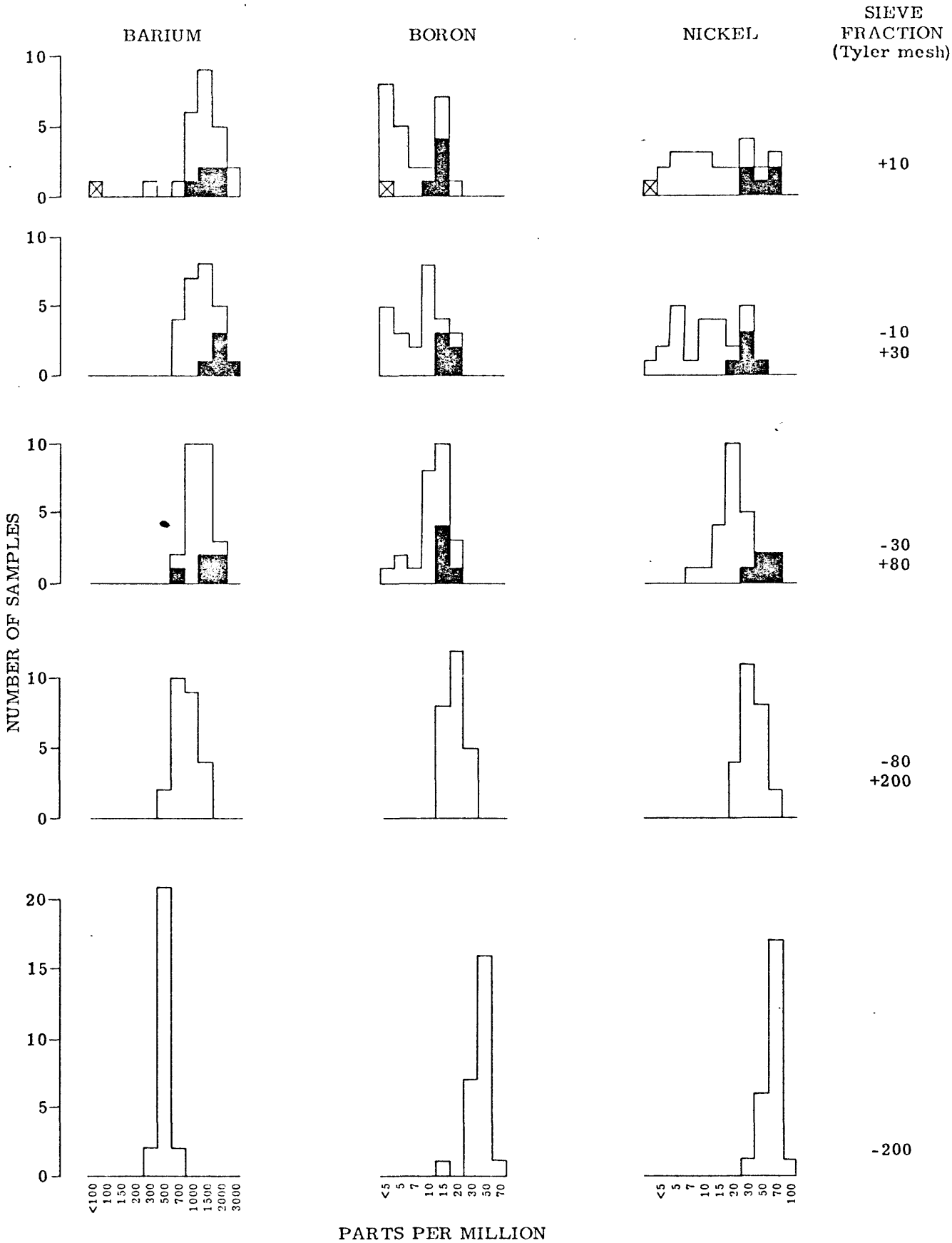

Figure 2. - Histograms of the barium, boron, and nickel content of surficial debris as a function of the size fraction. The median value changes progressively for the three elements as the grain size increases. Heavy shaded blocks in the three coarsest fractions represent samples from metasedimentary terrane south of the Uyaijah ring complex. The block marked X in the coarsest fraction is sample 60002.

We interpret this lack of variation to result from thorough aeolian introduction of fine debris from a huge area of Saudi Arabia.

Preceding to coarser fractions from this uniform fine fraction, the median value changes progressively and the range increases progressively for all 14 elements. The medians decrease with increasing grain size for 11 of the elements: boron, cobalt, chromium, copper, manganese, nickel, scandium, titanium, vanadium, yttrium, and zirconium. The medians increase with increasing grain size for three elements: barium, lead, and gallium. The samples from the Uyaijah ring structure are much richer in barium, lead, and gallium than the shield-wide average for like samples (Theobald, 1971). The samples from the Uyaijah ring structure contain about the same as or less than the shield-wide average contents for the elements that show a decrease with increasing grain size. These relations confirm our interpretation that the fine fractions are largely introduced aeolian debris and have no local significance.

The increase in the scatter of concentrations obtained with increasing grain size is interpreted to mean that the coarser the size range, the more local the area represented. This conclusion parallels the logic for rejecting bedrock samples, because bedrock would be the end point of increasing grain size. We were, therefore, faced with a choice of samples to represent the area to be sampled. On grounds that aeolian dilution has removed too much of the local variation, all fractions finer than 80 mesh have been rejected. The fraction coarser than 10 mesh was rejected as representative of too small an area. Samples 60002 illustrates the limited range of this fraction. This sample consists of coarse material that is almost

entirely resistant quartz from nearby veins, and the analysis of the quartz shows that it is remarkably free from trace elements. The geologic setting of the sample suggests that it is in an anomalous area and the anomaly is confirmed by results of analyses of finer fractions of the sediment and of the heavy-mineral concentrate. Clearly, use of the coarse fraction as a geochemical sample medium would lead to too erratic a distribution of elements to be useful at our sample spacing of 1 km.

The choice is thus limited to the two size fractions between 10 and 80 mesh. Both of these fractions were analysed through the remainder of the preliminary traverses with results similar to those presented for the original orientation traverse. Though we had hoped to use the 30 to 80 mesh fraction of the sediment to maintain compatibility with earlier work, the overall range in this fraction is not adequate to allow clear distinction among the rock types encountered (fig. 3). For the 10 to 30 mesh range, samples from single rock types clearly differ from the group mean by more than analytical variation. Furthermore, the only detectable tungsten in the unconcentrated surficial debris was in the 10 to 30 mesh fraction.

Neither molybdenum nor tungsten were present in the unconcentrated surficial debris in generally detectable amounts. The only reported metal was present at the limit of detection. By contrast, heavy-mineral concentrates from the original traverses range through an order of magnitude or more for both elements. Clearly, the heavy-mineral concentrates had to be retained as the primary sample for defining the anomaly in spite of the relatively high cost of sample preparation.

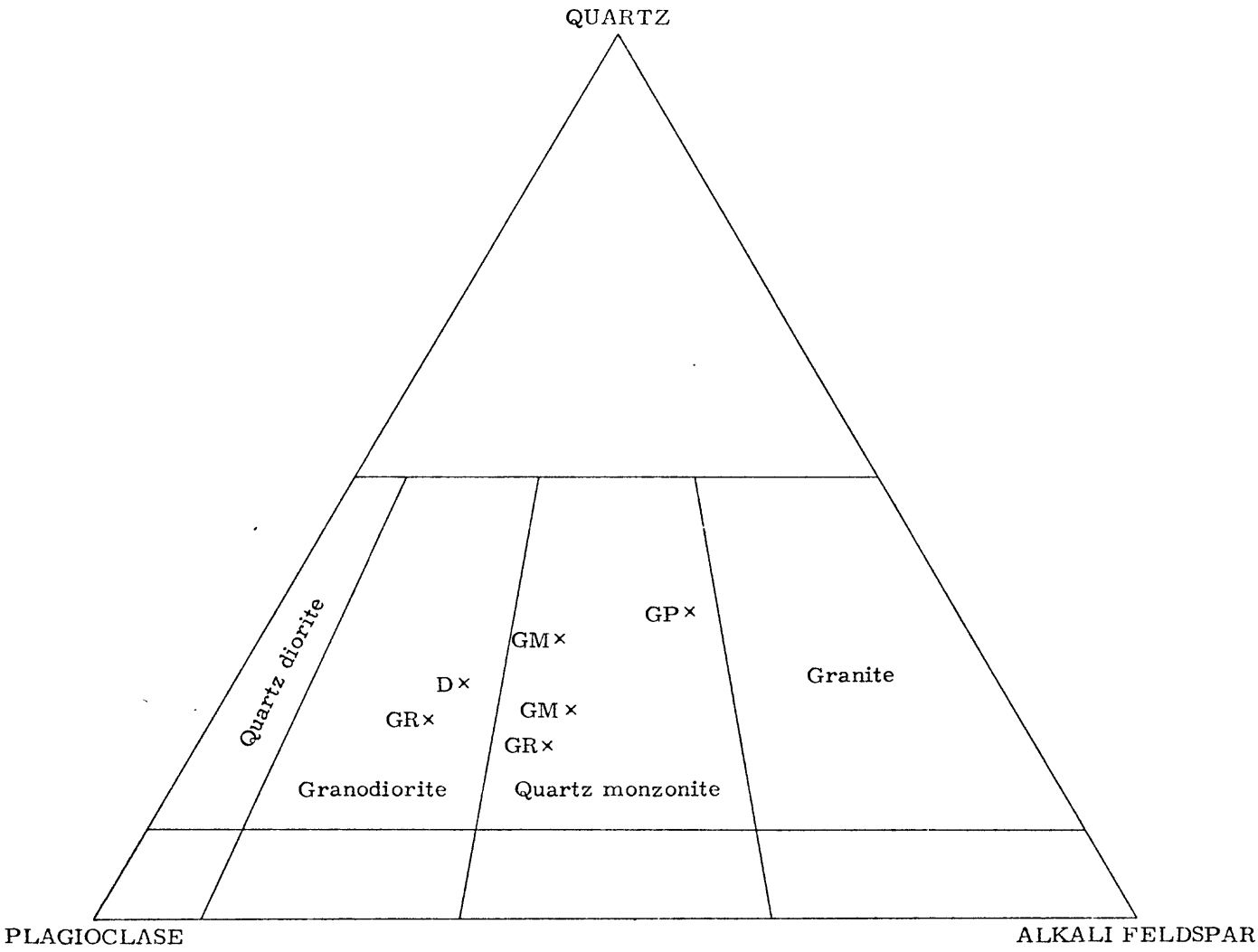

Figure 3.- Diagram showing composition of six rock samples from the Uyaijah ring structure. D - diorite; GR - porphyritic granodiorite; GM - quartz monzonite; GP - alkaline granite. Compositions determined by Abdul Malek Helaby by point counting stained slabs.

The tungsten content of heavy-mineral concentrates from the initial four traverses defined the Uyaijah ring structure as the primary target. Of the 62 samples collected, five contained more than 20 ppm tungsten. Four of these were from the altered and veined area of quartz monzonite at the center of the ring structure and one was near an altered zone intersected at the west edge of the ring structure. Tungsten was not found in samples from the long traverse acrossthe Kushaymiyah complex to the west of the Uyaijah ring structure, and no tungsten was present in samples taken on the traverse across the small intrusive to the south of the Uyaijah ring structure.

The geochemical orientation survey and interpretation of sample analyses indicated that the Uyaijah ring structure could be evaluated by sampling along traverses oriented parallel to the primary orientation traverse and separated at 1 km intervals. These traverses were laid out and 10 to 30 mesh sediment samples were taken along them at 1 km grid intersections, as were samples that were panned for heavy-mineral concentrates. More than 400 samples were taken in the ring structure, all that could be processed in the time allowable. The 1 km spacing precluded the use of rock samples for more than descriptive geologic information, since they would have been representative of too small an area within the grid.

GEOLOGY OF THE UYAIJAH RING STRUCTURE

The Uyaijah ring structure is here interpreted to be a nearly circular ring fracture system in sedimentary rocks of the Murdama Group and in two post-Murdama igneous rock bodies. The ring fracture system developed over a rising cyclinder of alkaline, quartz-rich granite that invaded both the fracture system and its host rocks.

A pre-existing, west-northwest-trending transverse fault zone was a weak feature that controlled initiation of the intrusion and later served with an east-trending fault system to accomodate minor strain release. Alteration and veining, with attendant tungsten and minor molybdenum mineralization, accompanied the intrusion of the alkalic granite in the ring fracture and also proceeded over cupolas on the rising cylinder in the central part of the complex. A variety of dike rocks invaded the complex, largely along the east-trending fractures, during and following alteration and veining.

The major rock types and their regional relationships have been described in the series of reports issued or to be issued by the BRGM on the Kushamiyah area (fig. 1). The following reports, in particular, provided much of the preliminary information that supported our effort:

(1) 66 JED 15, Eijkelboom, 1966, The mineral resources and geology of the Idsas-Wadi Jifr region (Sheet 117, Zone II).

(2) 68 JED 1, Vincent, 1968, Geology and mineral resources of the Halaban-Sabhah region (Sheet 118 - Zone II).

(3) 70 JED 6, Bois and Shanti, 1970, Mineral resources and geology of the As Sakhen quadrangle (Sheet 130).

(4) 70 JED 7, Leca 1970, Mineral resources and geology of the Jabal Sahah quadrangle, (Sheet 132 east).

(5) 70 JED 26, Lancombe and Letalenet, 1970, Mineral resources and geology of the Jabal Al Hawshah quadrangle.

Maps in various states of preparation are available at BRGM for the areas to the west and northwest of the study area. Readers are referred to these reports for details of the regional geology. The descriptions that follow pertain only to the geology of the Uyaijah

ring structure itself, shown on plate 2 and in part described on the explanation for that map.

Lithologic units

The 16 lithologic types recognized in the field can be classed into four general groups of rocks on the basis of composition, mode of occurrence, and time of emplacement. A structural discontinuity separates each of these major composite units from its predecessors, and these four units are the ones that appear on preceding maps of the area. From oldest they are: (1) Murdama Group rocks, (2) calc-alkaline granitic rocks, (3) alkaline granitic rocks, and (4) late dike rocks.

Murdama Group

Rocks of the Murdama Group mapped in the vicinity of the Uyaijah ring structure are confined to the outer-ring-fracture zone, to narrow septa between the southeast lobe of the Kushaymiyah complex and the Jabal Fahwah intrusive, and to the disturbed belt between the Kushaymiyah complex and the north-northwest-trending fault to the east. All metasedimentary rocks and associated, sheared amphibolites in these areas are included in the Murdama Group though deformation is often sufficiently intense to obliterate original textures and compositions of other rock units that may be present.

A wide range of sedimentary rock types may be recognized where metamorphism is least intense. Shales and siltstones predominate. These are interlayered with fairly clean sandstone, arkose, and wacke. Fine-grained conglomeratic units are common; the coarsest fragments rarely exceed fine pebble sizes. Coarse conglomerate that has been noted elsewhere near the base of the formation was not recognized. Float from carbonate-rich layers was seen in several places around the

southwestern part of the outer-ring-fracture zone. Amphibolite, presumably derived from igneous rocks, is fairly common south of tne ring structure.

Dynamic metamorphism appears to have dominated the reconstitution of these rocks. They are intensely sheared along anastomosing fractures usually only a few centimeters apart. The fractures are about parallel to adjacent igneous contacts and are nearly vertical in most places. South of the Uyaijah ring structure, at the greatest distance traversed from the igneous rocks, a marked flattening of the shearing concomittent with dimunition in its intensity was observed. Just to the south of the area mapped, questas exhibit little-deformed sediments dipping only 15 to 20 degrees south. A sizeable mass of amphibolite in the southern exposure of the Murdama appears to have a southeasterly outcrop pattern, oblique to the principal shear direction.

Recrystallization has affected most of the sediments. Hornfels is ubiquitous but differs markedly in intensity with proximity to sills of alkaline granite. Where shearing and intrusion are most intense along the southeast and east parts of the ring fracture, biotite-bearing gneiss exhibits marked metamorphic segregation in the form of boudin-like quartz seams. East of the Kushaymiyah complex where the sediments are interlayered with sills of the older of the calc-alkaline granite, recrystallization has often proceeded to phyllites or fine-grained muscovite or muscovite-biotite schist. The metamorphism in this area appears to have been more uniform and pervasive.

The metasedimentary rocks have yielded to dynamic stress exerted on the area and have absorbed most of the deformation.

Calc-alkaline igneous rocks

Three distinct phases of calc-alkaline intrusive rocks have been recognized in and around the Uyaijah ring structure. In sequence these are diorite, with associated gabbro, porphyritic granodiorite, and quartz monzonite with associated aplite. Though the porphyritic granodiorite reacted brittly to the intrusion of the quartz monzonite, there is no evidence for a regional tectonic event during emplacement of these three rock types.

Diorite, granodiorite, and gabbro.-- Diorite, granodiorite, and gabbro are present in several lobes of the Kushaymiyah complex and in the small intrusive to the south of the complex. The two areas of diorite shown on the map of the Uyaijah ring structure differ in composition and texture and probably represent different lobes of the complex, one to the west and one to the northwest of the Uyaijah ring. No attempt has been made to separate these rock units since they are all peripheral to the main ring and largely incidental to the discussion here. The most westerly lobe of the Kushaymiyah complex, crossed on one of the orientation traverses, appears to be largely granodiorite and diorite. The unit mapped as gabbro is confined to inclusions within the ring and probably represents either relics of the diorite assemblage or inclusions of these rocks.

Small- flat exposures of mottled purple and green, porphyritic coarse-grained rock crop out to the northwest of the outer ring. The porphyritic appearance, caused by selective weathering of feldspar and amphibole is lost on fresh surfaces. The rock consists of about 70 percent calcic plagioclase and 30 percent amphibole. Quartz, if present

is minor. Apart from albitic rims separating the amphibole and plagioclase near minor fractures, there is little evidence of metamorphism of the original igneous rock.

The larger outcrop area of diorite shown along the west side of the ring is generalized, as relations in this area are far too intricate and complex to be illustrated at the map scale. The dioritic rock is a coarse-grained, equigranular, dark-gray mixture of about equal proportions of plagioclase and amphibole. To this end member, biotite and quartz have been added at most localities in what appears to be a direct relationship to the amount of added alkalic feldspar. The alkalic feldspars are much coarser than those of the normal rock texture and resemble in all aspects those seen in the porphyritic granodiorite. At several localities the contacts with the porphyritic granodiorite are gradational. Owing to what appears to have been the secondary addition of alkalic feldspar, biotite, and quartz, the rock usually has the gross composition of granodiorite.

Mafic inclusions are common in the later calc-alkaline rocks in the core of the ring structure, and three of these are large enough to be shown on the map. Through reaction with the enclosing granitic rock they have become biotite and alkalic-feldspar-rich aggregates whose original compositions are hard to decipher. They appear, however, to be somewhat more mafic than the larger dioritic masses of adjacent lobes of the Kushaymiyah complex. The inclusions could be derived from any pre-existing, mafic rock but autolithic derivation from only slightly earlier members of the same igneous sequence seems more reasonable.

Porphyritic granodiorite.-- The term porphyritic granodiorite provides the most descriptive name for the predominant rocks of the calc-alkaline suite.

suite. Gross composition of the rock ranges from granodiorite to quartz monzonite. This rock underlies the outer part of the core of the Uyaijah ring structure, the southeast lobe of the Kushaymiyah complex, and the intrusive of Jabal Fahwah. It forms a lit-par-lit migmatite with sheared Murdama rocks east of the Kushaymiyah complex.

The rock is a coarse aggregate of biotite, plagioclase, and quartz in which is set a liberal quantity of crystals of alkalic feldspar up to 1-2 cm long. Both the biotite and alkalic feldspar are oriented, defining a weak to strong planar structure. The alkali feldspars are poikilitic with numerous inclusions of quartz, biotite, and plagioclase oriented along growth lines of the host feldspar. Relict amphibole is common in biotite aggregates and locally amphibole predominates over biotite. Sphene in coarse euhedral crystals is abundant and, particularly in the Fahwah intrusive, may constitute 1 percent or more of the rock.

Contacts with adjacent rock units take several forms and provide the major clue to the origin of the rock. In the lit-par-lit zone with the metasediments east of the Kushaymiyah complex, the contacts are sharp and no reaction is evident. Though the metasediments are intensely sheared, the sills and pods of porphyritic granodiorite are little deformed. Possibly these are competent pieces of granodiorite sheared in with the strain-absorbing sediments. It is more likely, however, that they are sill-like igneous intrusions into previously sheared sediments. The most reasonable relationship would be late syntectonic igneous intrusion of porphyritic granodiorite into intensely deformed sediments. In this interpretation, the porphyritic granodiorite is younger than the Murdama.

Gradational, metasomatic contacts between the porphyritic granodiorite and older, more mafic igneous rocks are exposed in the northwest corner of the Jabal Lahwah intrusive, along the east side of the southeast lobe of the Kushaymiyah complex, and along the west side of the Uyaijah ring structure. At these localities, dioritic rocks have sparse feldspar phenocrysts a meter or two away from the contact with porphyritic granodiorite. The zone of gradation from diorite with sparse secondary feldspar to good biotite-rich porphyritic granodiorite is abrupt, taking place through only a few centimeters. The dioritic rocks that have reacted cannot be positively identified as the preceding calc-alkaline intrusive phase along the east side of the southeast lobe, but this seems likely because there is no evidence for metasomatic reaction with diorites in the Murdama at other localities. If, as we infer, the metasomatic reaction producing the alkalic feldspar-rich granodiorite took place only with the next preceding calc-alkaline intrusive phase, then the time and nature of the reaction is simply explained. Late in the intrusive history, while still hot and probably still plastic, these dioritic cupolas reacted with their own potassium-rich residual fluids to produce the porphyritic granodiorite. This process was terminated and the mass was capable of brittle fracture before the next intrusive episode.

Quartz monzonite and aplite.-- Two bodies of quartz monzonite have been mapped; one forms the core of the Uyaijah ring structure and the other the east lobe. Smaller dikes of quartz monzonite are peripheral to the central mass of the Uyaijah ring structure and small bodies of quartz monzonite are present along a broad east-trending zone that extends from the east lobe across the Uyaijah ring structure to the

west limit of the mapping. These bodies have a pronounced preference for east- or west-northwest trending fractures, indicating that these breaks were available for tensional opening before intrusion of the quartz monzonite.

The rock is a very ordinary, light-gray, medium-grained, equigranular, weakly foliated biotite-quartz monzonite. Foliation is defined by weak alignment of biotite. Sparse hornblende is almost completely replaced by biotite. Minor accessories are opaque minerals, apatite, and rare zircon.

Contact relations with the older porphyritic granodiorite are sharp. There is no deformation of the invaded rocks, and there are no recognizable contact metamorphic effects. The east lobe is evidently a plug because its southern contact with the lit-par-lit mixture of porphyritic granite and metasediments is linear, nearly vertical, and almost perpendicular to the foliation of the older rocks. The east lobe has minor irregularities in its outer contact, but it contains few inclusions of the invaded rocks. By contrast, the lobe of quartz monzonite in the core of the Uyaijah ring structure was emplaced by stoping. The boundary of this lobe was drawn subjectively between porphyritic granodiorite cut by quartz monzonite and quartz monzonite with numerous rectangular inclusions of porphyritic granodiorite. The zone of stoping is as much as 1 km wide and completely surrounds the central mass of relatively clean, inclusion-free quartz monzonite.

Aplite dikes are commonly associated with the quartz monzonite and intrude either the quartz monzonite itself or more commonly, the porphyritic granodiorite near the contact with quartz monzonite. Only the conspicuous aplite dikes or dike swarms have been mapped.

Alkaline granite suite

The four related rocks that make up this suite are sparingly present as dikes, pods, or irregular masses throughout the area. They are most abundant as sills in the ring-fracture zone and as dikes in the core of the central ring and near the middle of the southeast lobe of the Kushaymiyah complex. These dikes cut all preceding rocks and are cut by all succeeding rocks; thus, the age relations are fixed. Within the suite, contacts are gradational, and distinction among the rock types is largely made on a basis of texture. A dike of granite, for example, may become narrow and finer grained until its texture changes to that of rhyolite. It may then terminate in a pod-shaped mass of quartz or pegmatite.

Granite is by far the most abundant rock in the suite. It forms the major sills along the south and southeast parts of the ring-fracture zone. The granite is a medium- to coarse-grained, pink mixture of discrete grains of alkalic feldspar, quartz, and plagioclase, with biotite as a varietal mineral. Perthite is common both in discrete grains and as reaction rims between feldspar grains. Opaque minerals, apatite and sphene, are accessories. Biotite is extensively altered to chlorite and plagioclase to sericite, evidencing a possible active deuteric phase.

The rhyolite is a fine-grained version of the granite that ranges from microgranite, almost an aplitic textured rock, into an aphanitic pink dike rock. Volatiles were probably common in the rhyolites, because the wall rocks along even narrow dikes are altered. Feldspar phenocrysts of the porphyritic granodiorite may be reddened for 1 m or more on either side of rhyolite dikes, which are not over a few

centimeters thick.

Pod-shaped masses of pegmatite and quartz are scattered along the southern part of the ring fracture, within and on both sides of the fracture. The pegmatites are zoned with massive quartz cores surrounded by pink, intensely cleaved alkalic feldspar.

The alkaline granite sills permeate the ring fracture as an almost continuous set of sheets. Although weakly to moderately foliated, the sills are not themselves sheared. The foliation is a primary flow foliation. There is no evidence that the ring fracture precedes the alkaline granite. It appears most likely that the west-northwest-trending fault through the ring was active as a transverse fault after emplacement of the quartz monzonite and before the period of ring fracturing.

The abundance of dikes of alkaline granite near the center of the ring core suggests a shallow cupola of alkaline granite beneath this area. The abundance of alteration and quartz veining in this same area adds weight to the suggestion of a cupola, and the abundance of lanthanum in concentrates from this area again identifies the alkaline granite as the prime source of metal in the cupola. We interpret these time, space, and structural relations to mean that the Uyaijah ring structure is a circular stock of alkaline granite that has not yet been unroofed by erosion. The ring fracture is the glide plane along which the intrusion rose and the core of the ring is the plug being forced up ahead of the intrusion. The diagramatic cross section accompanying the geologic map (plate 2) illustrates this interpretation.

Quartz veins and alteration

Quartz veins follow alkaline granite in time, but have a remarkably similar distributive pattern within the ring structure. They precede most if not all of the postgranite dikes in time. Though the quartz veins form a separate depositional episode, most likely tney represent the last phase of the alkaline granite suite so they are discussed here as a separate group rather than including them with the later dike systems.

The quartz veins are fracture fillings usually of several generations of coarse crystalline quartz. Comb structures are common and the broken cross sections of single crystals exhibit repeated growth stages as euhedral color zonation. Where veins are filled completely, color zonation commonly defines earlier comb structure from free-growing crystals. In some veins the quartz is more massive and locally almost chert-like. Chalcedonic quartz is uncommon and confined to vein walls or thin seams. Pyrite is the most common accessory mineral readily recognized. It occurs in euhedral cubes up to 2 cm on a side. Usually it contains several tenths of a percent molybdenum. Coarse flakes of molybdenite are occasionally seen and chalcopyrite is rare. Secondary copper minerals are fairly common along vein walls. Yellowish-tinted, white-fluorescent scheelite can be found in more massive quartz seams in the core of the ring and along the ring fracture, but the distribution of this mineral is poorly known from direct observation because of its great similarity in white light to the enclosing quartz. Single scheelite crystals are as much as 1 X 2 cm in cross section.

Single quartz veins range from thin films to more than 1 m in width. Single veins may persist along strike for more than 1 km, but

strike persistence is most commonly maintained by echelon swarms of individual veins that persist on the order of tens or hundreds of meters. Vein swarms are common, and in the core of the ring the veins may constitute 10 percent or more of the rock for widths of hundreds of meters. The veins rarely form stockworks but instead have a pronounced preference for east-trending fractures with a somewhat less strong orientation along the west-northwest trend of the transverse fault. The preferred orientation is parallel to that of the alkaline granite dikes within the ring and many of the dikes are bordered or internally laced by anastomosing quartz veins.

Alteration is most intense in the area of maximum quartz veining and particularly along the west-northwest-trending fault zone. Silica introduced with the quartz veins has locally added to the alteration, but in general the shattering and argillization most characteristic of the altered zones is independent of the quartz veins and vice versa. Evidently the altering solutions and the silica-rich solutions occupied about the same area at about the same time, but they evolved relatively independently. Where single quartz veins are encountered away from the main zones of alteration in the porphyritic granite, alteration of the vein walls may be conspicuous. This alteration takes the form of reddening of the feldspar phenocrysts of the granite, is almost identical to the alteration adjacent to the rhyolite dikes, and strengthens the inferred tie between the quartz veins and the alkaline granite suite.

Two zones of intense quartz veining near the center of the quartz monzonite in the center of the ring are separated by the zone of intense shattering and alteration along the transverse fault. Inasmuch

as these zones are of prime interest in the discussion of economic geology, we have given them names: the North Vein System north of the transverse fault and the South Vein System south of the transverse fault. These vein systems are inferred to be leakage from a cupola of an underlying alkaline granite mass.

Late dike rocks

The east-trending faults have hosted two sets of dike rocks that record the youngest intrusive events to effect of the area. Both sets are fine grained, largely aphanitic, rocks and, in the absence of chemical and petrographic data, cannot be accurately placed in a rock classification system. Largely on a basis of color, the earlier set of dikes is lumped under the term andesite and the later set is lumped under the term dacite.

The andesite dikes are dark gray to black, aphanitic to porphyritic rocks commonly with phenocrysts of plagioclase and a mafic mineral. Small inclusions of a great variety of other rock types are common. The dikes are usually about 1 m thick but range from a few centimeters to several meters in thickness. The dikes crop out in two patterns that probably reflect two or more types of rock and probably two or more ages of intrusion. An earlier, sheared, mildly altered, erratically oriented and discontinuous set of dikes appears to be syncronous with or slightly earlier than the quartz veins. Some of these dikes may be lamprophyres as suggested by Whitlow (1971). They rarely have continuity for more than 1 km and have not been seen cutting the ring fracture. The younger set is composed of little altered, more regular, longer dikes that, as interlacing, echelon swarms, maintain continuity for tens of kilometers. Comb quartz veins that form walls to these dikes frequently exhibit

overgrowth of clear, glassy quartz as is common on milky white quartz crystals of the vugs suggesting recrystallization of the quartz at the time of emplacement of the dikes. These dikes commonly cut the ring fracture, which may be offset along them.

The dacite dikes are brown to reddish-brown porphyritic aphanites with phenocrysts of glassy quartz and feldspar. Small inclusions of a variety of other rocks are commonly present. Alteration is slight. The dikes are regular and single dikes are continuous for distances of 10 km or more. Two dike systems have been recognized. One begins near the center of the ring core, on the north side of Jabal Thaaban, and extends as a single dike due east to the ring edge. To the east, it is exposed as an echelon set across the ring fracture and beyond the area of mapping. The other is a braided mesh of dikes that begins in the southeast corner of the core of the ring and extends west across the core and the ring-fracture zone into Murdama rocks. Both dike systems truncate, distort, or offset the through-going andesite dike swarms. The dacite dikes are the youngest bedrock unit that has been recognized.

Structure

The structural pattern is dominated by shear tectonics. Four stages of shearing, each with a characteristic pattern, are recognized. Older structural entities have been reactivated during younger deformations or have served to divert younger trends.

The oldest period of shearing trends north-northwest along the easternmost edge of the map. Rocks of the Murdama Group are sheared along this trend and porphyritic granodiorite either was injected into these shears in lit-par-lit fashion or was sheared in with the Murdama.

The more likely of these alternatives is intrusion of the porphyritic granodiorite into already sheared Murdama, because the granodiorite is not itself sheared. However, the possibility that the granodiorite behaved as a competent body while the Murdama absorbed the major motion and provided lubricant during shearing cannot be eliminated. The east lobe of quartz monzonite cleanly truncates rocks sheared during this deformation, thus setting an absolute upper limit to the time of deformation. The sheared rocks are parallel and adjacent to a major north-northwest-trending structural break clearly evident in the aeromagnetic data just to the east of the area mapped. This break has not been recognized and mapped in the field. It must, however, be a fault.

Nearly east-trending faults are common within the ring structure; they cut the outer ring fracture. Most of the dike rocks emplaced in the area, from the quartz monzonite to the late dacite dikes, are along these fractures. The presence of quartz monzonite dikes along this trend indicates a very early tensional release on what must have remained a relatively fixed tensional direction throughout later evolution of the regional structure. This fracture system provided the major avenues for alteration and the introduction of vein quartz. The principal motion on the fault set appears to have coincided with the introduction of quartz, because quartz-filled fractures of this set offset the ring fracture. Still later fractures of the set, filled by andesite dikes, are deformed into the pattern of the transverse fault, and dacite-filled fractures of the set are deformed at the ring fracture.

A west-northwest-trending shear zone bisects the Uyaijah ring structure axially. To avoid obscuring other mapped entities this shear zone has not been shown on the geologic map (plate 2); however,

its position is reflected by the pattern of alteration and dike rocks. Its physiographic expression is marked by a prominent lineation of topographic features and its magnetic expression is fairly clear. The first activity along this fault zone appears to be left-lateral transverse faulting that offsets the sheared mixture of Murdama and porphyritic granodiorite at the east edge of the map and appears to offset the contact between quartz monzonite and porphyritic granodiorite in the core of the ring. The quartz monzonite is intensely sheared along this zone, but dikes of alkaline granite are common in the zone, thus bracketing its initiation. The fault zone was reactivated after formation of the ring fracture, shattering alkaline granites implaced in the zone and offsetting the ring fracture; however, this latter motion produced apparent left-lateral motion of the ring fracture and apparent right-lateral motion of its contained alkaline granite sills. Evidently the late movement was largely vertical rather than transverse. The transverse motion on the fault zone appears to have offset the principal quartz vein systems in the core of the ring, providing the present separation of the North and South Vein Systems. However, there is no evidence that the quartz of the veins has been sheared along the fault zone and quartz veins occur in the fault zone. If the transverse fault zone did offset the large quartz vein systems, it is most likely that it offset the fracture system before the introduction of the quartz. This fault zone has the same trend, age, and principal offset pattern as the major west-northwest-trending Najd Fault to the south and its counterpart to the north.

The ring-fracture zone that serves as host to the alkaline granite sills surrounds the Uyaijah ring and constitutes the outer ring of the complex. The zone postdates transverse motion on the west-northwest-trending fault zone but predates the alkaline granite and the late movement on both the west-northwest-trending fault zone and the east-trending faults. It is characterized by intense shearing, particularly of the metasedimentary rocks, along vertical shear planes often obliterating earlier structures. The intensity of shearing diminishes away from the ring edge and just to the south of the mapped area the sedimentary rocks have gentle dips. Motion on the ring fracture zone is vertical with the core of the ring moving upward relative to the perimeter. The ring fracture zone is interpreted to be the bounding fault that facilitated the vertical rise of a near circular stock of alkaline granite. The principal evidence for the nature of the underlying mass is the nearly continuous swarm of alkaline granite sheets that have permeated upward along the fracture zone.

Summary of geologic history

Originally nearly horizontal sedimentary rocks of the Murdama Group were intensely sheared along a vertical, north-northwest-trending fault just to the east of the area mapped. The sheared sediments along with their less disturbed counterparts to the west were invaded by diorite to granodiorite magmas that late in their history of cooling developed large phenocrysts of microcline. Intrusion was lit-par-lit in the sheared rocks and most likely by more passing doming in the less deformed rocks to the west. Upon cooling of the porphyritic granodiorite to a brittle mass, tension was released along east-trending

fractures, a condition that was maintained through the remainder of the tectonic history. Quartz monzonite magma was intruded by vertical injection in the east lobe and by stoping in the core of the ring, the intrusions being facilitated by the east-trending tensional weakness. Tension continued as the quartz monzonite became brittle and a fracture system developed near the middle of the large intrusive. Major transverse faulting to the north and south of the area gave rise to a minor, west-northwest-trending fault zone that cut the complex axially and offset the rock units 0.5 to 1 km in a left-lateral sense. A volatile-rich, alkaline granite magma rose into the area along a nearly circular ring fracture. Sheets of the granite escaped along the bounding fracture zone and over a cupola developed beneath the sheared rocks in the middle of the quartz monzonite. As this magma cooled, the remnant volatiles altered accessible rocks along the transverse fault zone and in the sheared core, and large quantities of quartz filled the fractures. Lamprophyric rocks intruded the east-trending tensional openings. Minor, later, vertical adjustments took place along pre-existing west-northwest fractures of the transverse fault zone and along east-trending tensional fractures. Finally, the tensional fractures reopened to accomodate andesite dikes and later dacite dikes.

GEOCHEMISTRY OF THE UYAIJAH RING STRUCTURE

General features

Analytical data used to described the geochemical features of the Uyaijah ring structure were established by chemical and spectrographic analysis of panned concentrates from which the magnetic fraction had been removed, and by spectrographic analysis of a 10 to 30 mesh sample of surficial debris. The panned concentrate was used as a sample medium

for the colorimetric analysis (thiocyanate method) of tungsten and molybdenum, and was the medium for data relating bismuth to the anomalous tungsten areas and lanthanum to the alkaline granite. The sieved 10 to 30 mesh samples of surficial debris served primarily to establish the general geochemical features of the area.

The two analytical techniques used in analysis of the samples from the Uyaijah area resulted in sets of logrithmic-based data points; that is, the techniques themselves are based on a law relating optical density to concentration which is logrithmic in nature. The spectrographic technique is a 6-step semiquantitative method in which reporting points are 1, 1.5, 2, 3, 5, and $7x10^n$, where n is an interger used to determine the order of magnitude. This is a geometric progression with a factor of about 1.47, the 6th root of 10, between reporting points. The colorimetric technique used a geometric factor of 2 between standards, which gives a factor of 1.5 between reporting points if the mid-point between two standards is used to estimate an analytical value. Analytical data obtained by techniques that are not arithmetric in their reporting system may themselves affect the parameter of frequency distribution for a given element. One area in which data may be affected is in the application of normal statistical analysis to lognormal distribution. The usual techniques applied to data for determination of precision and accuracy are the calculation of the arithmetic mean and standard deviation. Calculation of a geometric mean and log-standard deviation, however, may give more valid parameters, but the geometric mean and log-standard deviation are not as familiar as their arithmetic counterparts and are somewhat more difficult to relate to the data.

Table 1 illustrates the precision and accuracy of semiquantitative spectrographic data presented in geometric steps. The percentage of replicate analyses which fall within plus or minus one geometric factor (step) from a selected standard value is given as an index of the precision or accuracy. This index can be compared from sample group to sample group and element to element.

The precision and accuracy indices for the Uyaijah samples are based on analysis of the standard rocks G-1, G-2, and GSP-1, chosen for their compositional similarity to the Uyaijah samples. The precision indices of all elements with determinable values exceeds 80 percent, except for magnesium in G-2 and GSP-1, chromium in G-1, and yttrium in G-1 and G-2. The less precise distribution of chromium and yttrium is believed to be related to the increased variation near the analytical limit of the spectral line used for determination of concentration. The variation in magnesium is probably due to difficulty in reading the spectrogram because of the broadening of the magnesium line. Accuracy of analyses is not as important in a geochemical exploration program as is precision, nevertheless it is worthwhile to note some apparent bias in the data. In addition to bias due to lack of precision for magnesium, chromium, and yttrium, a negative bias exists for beryllium in G-2 and molybdenum in G-1, and a positive bias exists for lanthanum in G-1 and gallium in G-2.

The precision of the colorimetric analyses as well as the relationship of the analytical variation to the total variation was investigated by analyses of 22 samples from one geographic location. In figure 4, curve A is a plot of the cumulative frequency vs log ppm tungsten.

Table 1. Precision and accuracy of 6-step semiquantitative analyses based on replicate analyses of standard rocks G-1, G-2, and GSP-1.

		ELEMENT[1]	Fe	Mg	Ca	Na	B	Ba	Be	Co	Cr	Cu	Ga	La
PRECISION	G-1	Median	1[2]	0.2	1	3	<5	1000	2	<5	7	15	50	100
		Percent replicates ± 1 step	100	100	94	100	N[3]	94	88	N	56	88	94	100
	G-2	Median	1.5	0.5	2	3	<5	2000	1	7	<5	10	50	70
		Percent replicates ± 1 step	100	62	86	100	N	100	86	93	N	100	93	93
	GSP1	Median	3	0.7	2	3	<5	1500	<1	10	<5	50	30	200
		Percent replicates ± 1 step	91	73	100	100	N	91	N	100	82	91	100	100
ACCURACY	G-1	Accepted value	1.5	0.2	1	2	1.5	1000	3	2	10	15	N	150
		Percent replicates ± 1 step	94	100	94	81	N	94	88	N	50	88	N	50
	G-2	Accepted value	1.5	0.5	1.5	3	N	2000	2↓3	5	5	10	20	70
		Percent replicates ± 1 step	100	62	86	100	N	100	14	93	N	100	31	93
	GSP1	Accepted value	3	0.5	1.5	2	N	1000	<2	7	15	50	10↓20	150
		Percent replicates ± 1 step	91	64	82	91	N	91	N	55	9	91	N	100

Table 1. Precision and accuracy of 6-step semiquantitative analyses based on replicate analyses of standard rocks G-1, G-2, and GSP-1. (Cont'd.)

	ELEMENT[1]		Mn	Mo	Nb	Ni	Pb	Sc	Sn	Ti	V	Zr	Y
PRECISION	G-1	Median	300	3	20	<5	50	<5	<10	1500	20	200	15
		Percent replicates ± 1 step	94	88	100	N	94	N	N	100	100	94	69
	G-2	Median	300	<2	<20	<5	30	<5	<10	3000	70	300	10
		Percent replicates ± 1 step	100	N	N	N	93	N	N	100	86	93	77
	GSP1	Median	300	<2	20	7	50	5	10	3000	100	300	30
		Percent replicates ± 1 step	91	N	100	100	82	100	100	91	91	100	100
ACCURACY	G-1	Accepted value	200	7	20	1	50	3	5	1500	20	200	20
		Percent replicates ± 1 step	100	12	100	N	94	N	N	100	100	94	62
	G-2	Accepted value	200	<2	10 ↓ 20	<5	30	5	<20	3000	50	300	<20
		Percent replicates ± 1 step	85	N	N	N	93	N	N	100	77	93	N
	GSP1	Accepted value	300	<2	20 ↓ 30	7	50	7	10	3000	30 ↓ 70	500	20 ↓ 50
		Percent replicates ± 1 step	91	N	N	100	82	73	100	91	N	100	N

1/ Concentrations are in parts per million except for Fe, Mg, Ca, and Na which are in percent.

2/ Accepted values are rounded to the nearest spectrographic reporting point. These values have been obtained from a variety of sources but primarily Fleishcher (1965) and Flanigan (1967).

3/ N = no data or indeterminant.

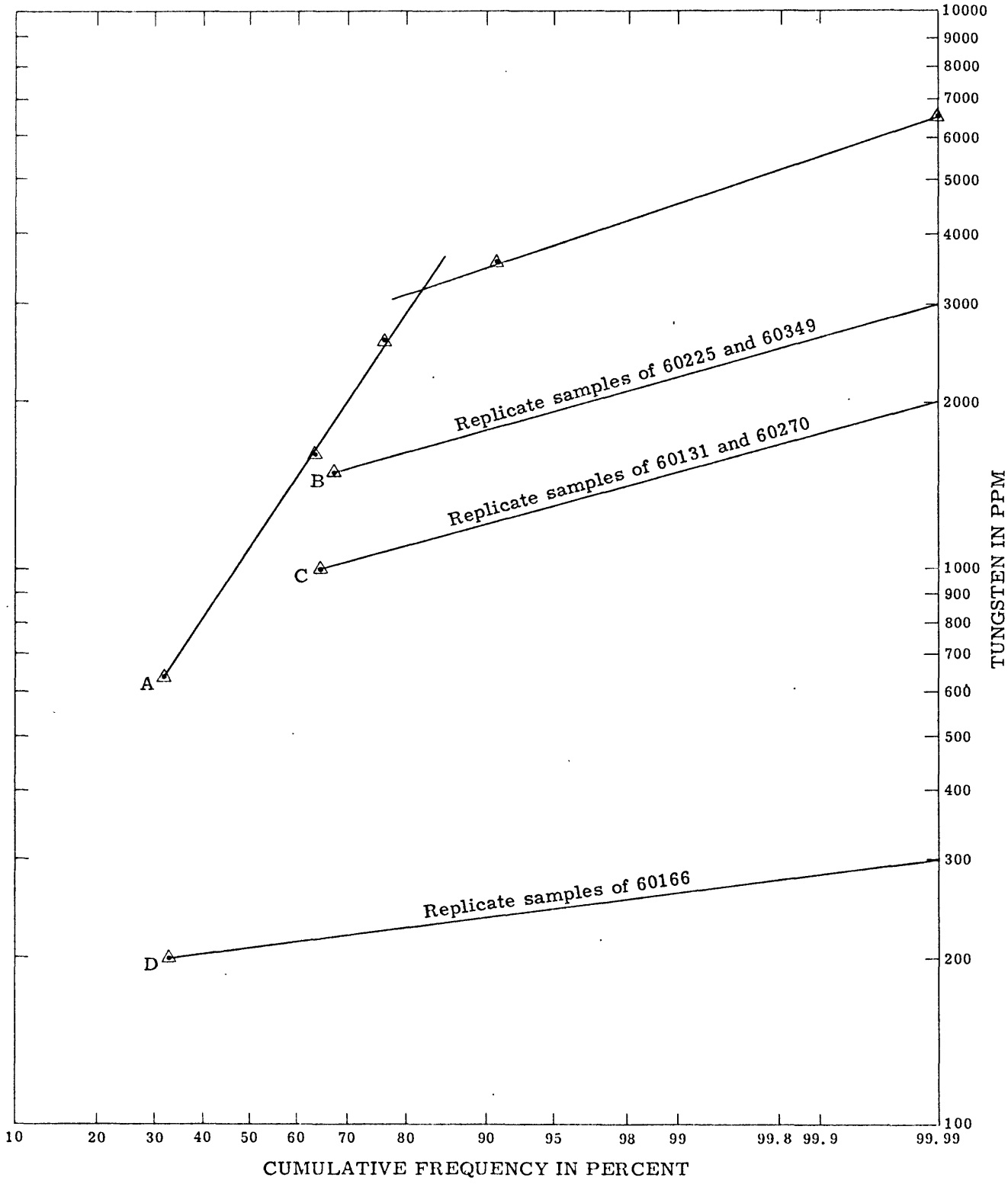

Figure 4.- Cumulative frequency vs log ppm tungsten for samples from location 60041.

There is a sharp break in the slope of this curve between 80 and 90 percent. The left portion of the curve illustrates the total variation present that is the natural variation at the sample site, the sampling variation and the analytical variation. The right portion of the curve illustrates the analytical variation of the maximum tungsten content determined at the sample site, as it is apparently a member of a family of curves (B, C, D) which represents replicate analyses of single samples from the site. These replicate analyses for tungsten show that 100 percent of the replicates are within a factor of 1.5 of the median.

A set of analytical data from Uyaijah was prepared for the application of a number of computer procedures programmed for the reduction and evaluation of geologic data by the STATPAC system of the U. S. Geological Survey. The initial input to the computer was the results of several types of analyses of a set of 448 samples. Each sample was analyzed spectrographically for iron, magnesium, calcium, titanium, manganese, silver, arsenic, boron, barium, cobalt, chromium, copper, lanthanum, molybdenum, niobium, nickel, lead, antimony, scandium, tin, vanadium, tungsten, yttrium, zinc, zirconium, sodium, and gallium, and colorimetrically for molybdenum and tungsten. The data set also included the locations of the samples by x-y coordinates. This data matrix was subdivided into one set of 408 samples covering the geochemical grid system over the Uyaijah ring structure and a second set of 22 samples representing the data from one sample location. These subsets were subsequently treated by various statistical techniques.

The data subset representing the 22 samples from one sample location were summarized by a programmed analysis in which the raw data

were reduced to the range, arithmetic mean, and the standard deviation (table 2). The variables lanthanum, molybdenum, niobium, tin, and zinc were eliminated from the statistical analysis because of lack of determinant analytical values or lack of variation. A bias is present in the parameters for yttrium, tungsten (spectrographic), scandium, lead, beryllium, and boron because the large number of indetminant values in the data set. The coefficient of variation suggests that the data for tungsten and molybdenum, and perhaps the data for magnesium and vanadium, could be treated by other types of statistical theory, but the arithmetic treatment here is valid.

The data subset representing the geochemical grid system was treated by graphical analysis of the raw data, replacement of the indeterminant values in the subset by determinant values, log transformation of the analytical values, graphical analysis of the transformed data, elimination of variables based on evaluation of the graphical analysis, contour printing, factor analysis, and contour plotting of the remaining variables.

The evaluation of the frequency distributions obtained in the graphical analysis of the log transformation of the data set resulted in the 16 variables iron, magnesium, calcium, titanium, manganese, boron, barium, cobalt, chromium, copper, nickel, scandium, vanadium, yttrium, zirconium, and colorimetric tungsten being retained for further treatment.

The areal distribution of each of the 16 elements was obtained by computer plotting and contour printing. A number of the maps of element distributions in samples of 10 to 30 mesh surficial debris obtained by the plotting are shown in figures 5 through 19. It was established from these maps that some distributive patterns for the elements could be related in a general way to the major rock units in the Uyaijah ring

Table 2.-- Range, mean, and standard deviation of 21 elements based on analyses of 22 samples from sample location 60041.

Element	Maximum	Minimum	Mean	Standard deviation
		Percent		
Fe	1.5	0.5	1.0	0.3
Mg	0.7	0.2	0.3	0.15
Ca	3.0	1.0	1.5	0.5
Ti	0.3	0.15	0.2	0.05
Na	5	3	3	0.9
		Parts per million (ppm)		
Mn	300	100	200	50
B	10	5	7	2
Ba	1000	100	700	200
Be	3	1	1.5	0.8
Co	10	7	8	1.5
Cr	30	5	15	6
Cu	15	5	10	3
Ni	20	5	15	5
Pb	30	20	20	3
Sc	7	5	6	1.0
V	70	20	50	20
W	300	100	150	100
Y	20	5	10	5
Zr	300	70	150	50
Ga	30	15	20	6
Mo	12	2	5	3.2
W	6000	150	2100	1700

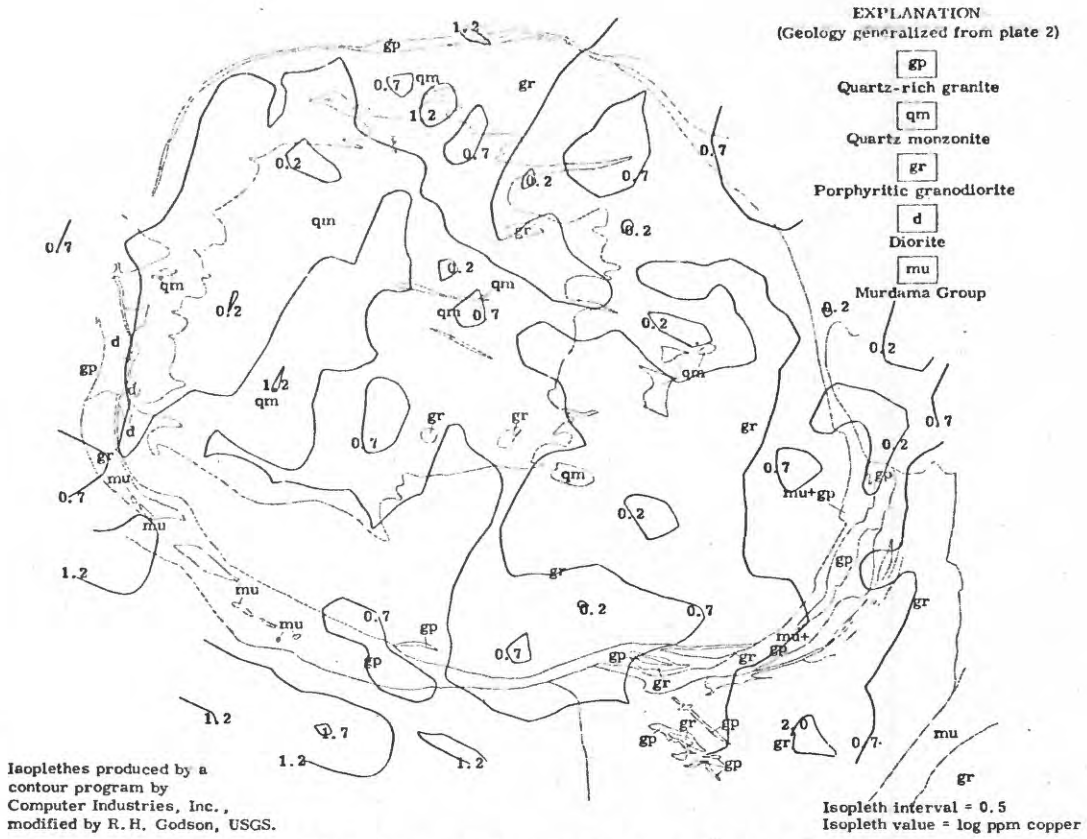

Figure 5.- Distribution of copper, Uyaijah *ring* structure.

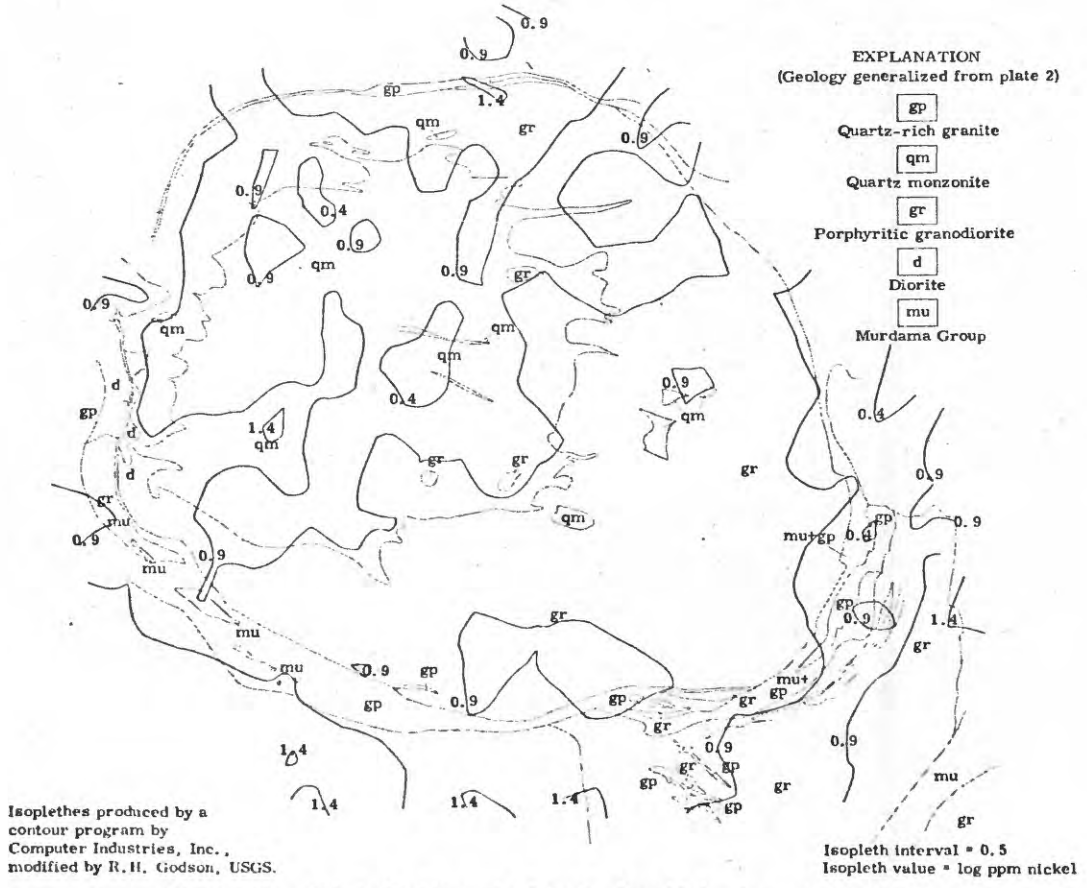

Figure 6.- Distribution of nickel, Uyaijah ring structure.

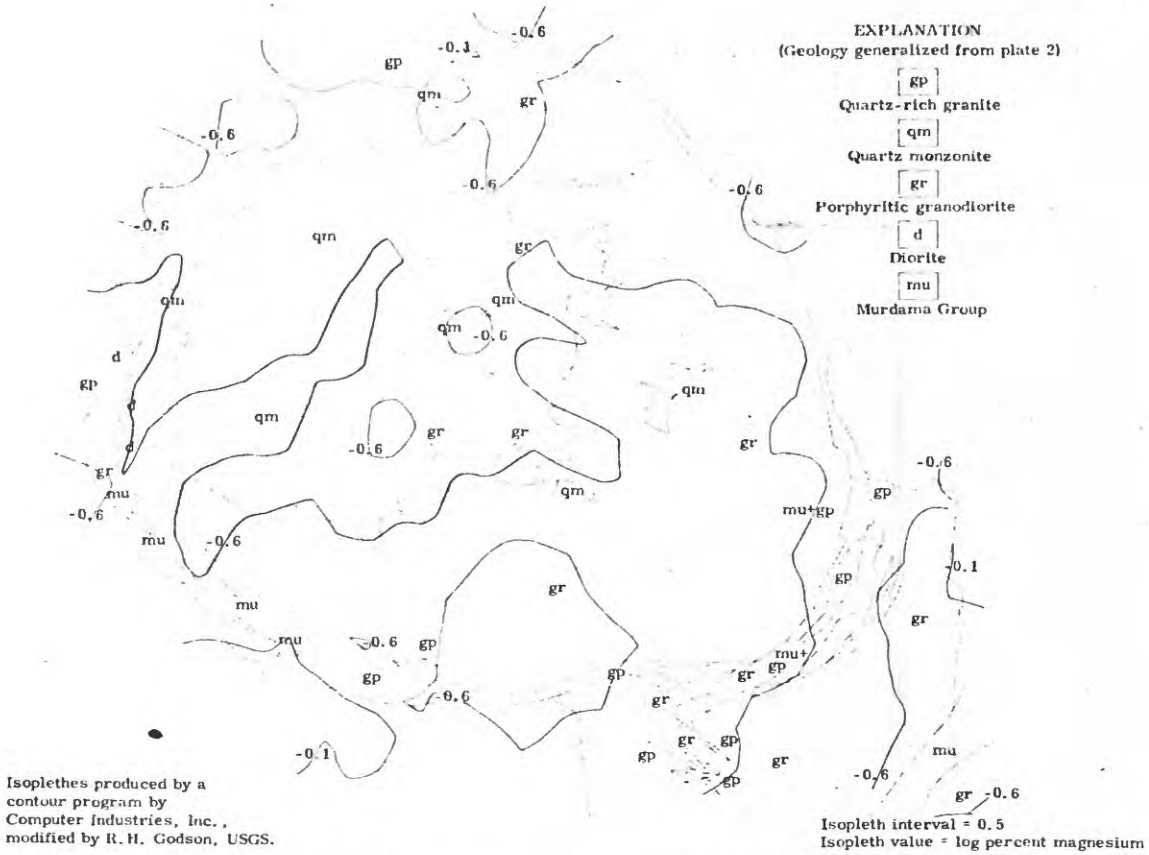

Figure 7.- Distribution of magnesium, Uyaijah ring structure.

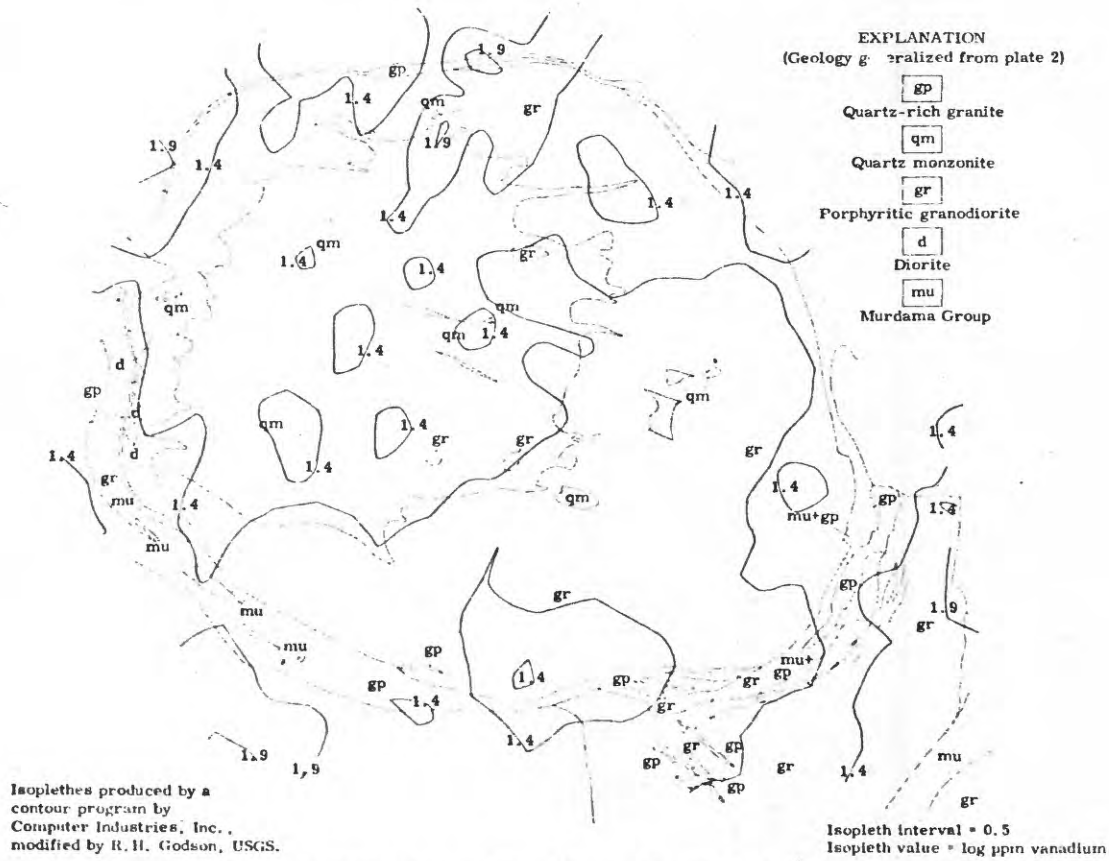

Figure 8.- Distribution of vanadium, Uyaijah ring structure.

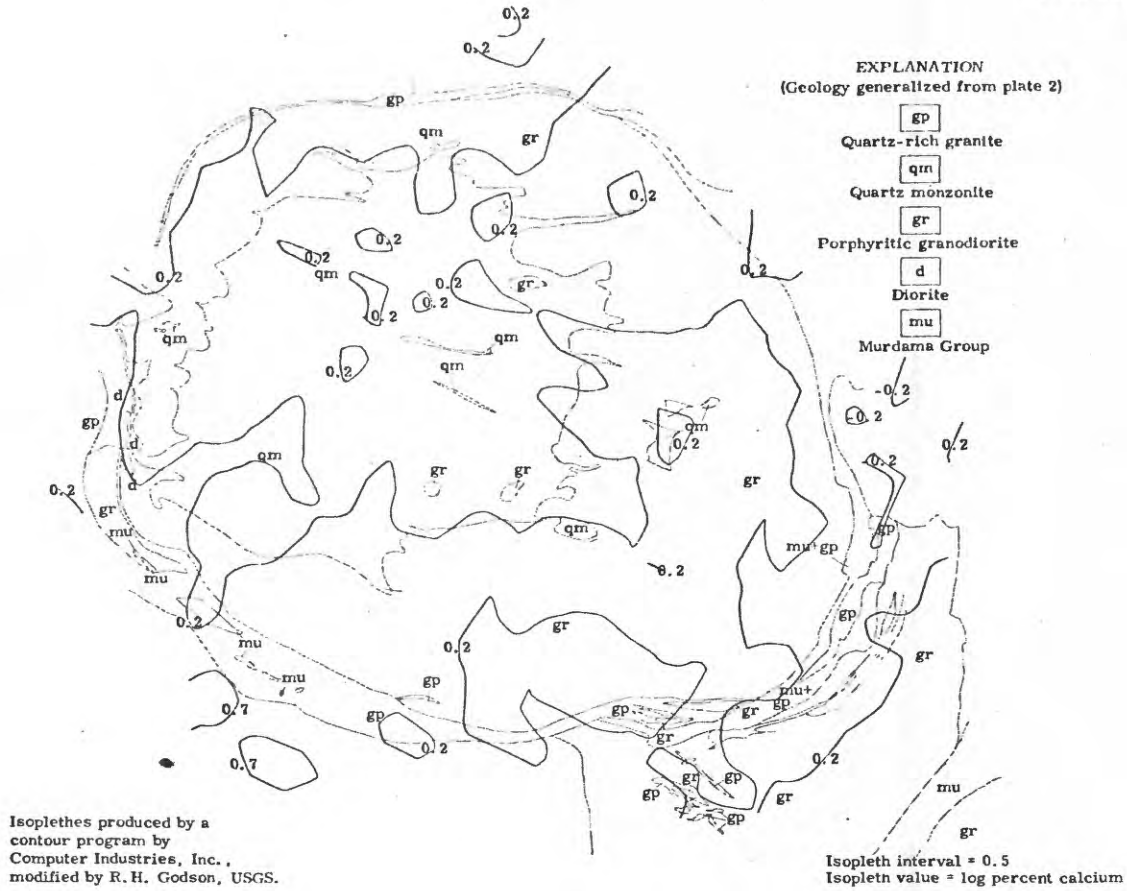

Figure 9.- Distribution of calcium, Uyaijah ring structure.

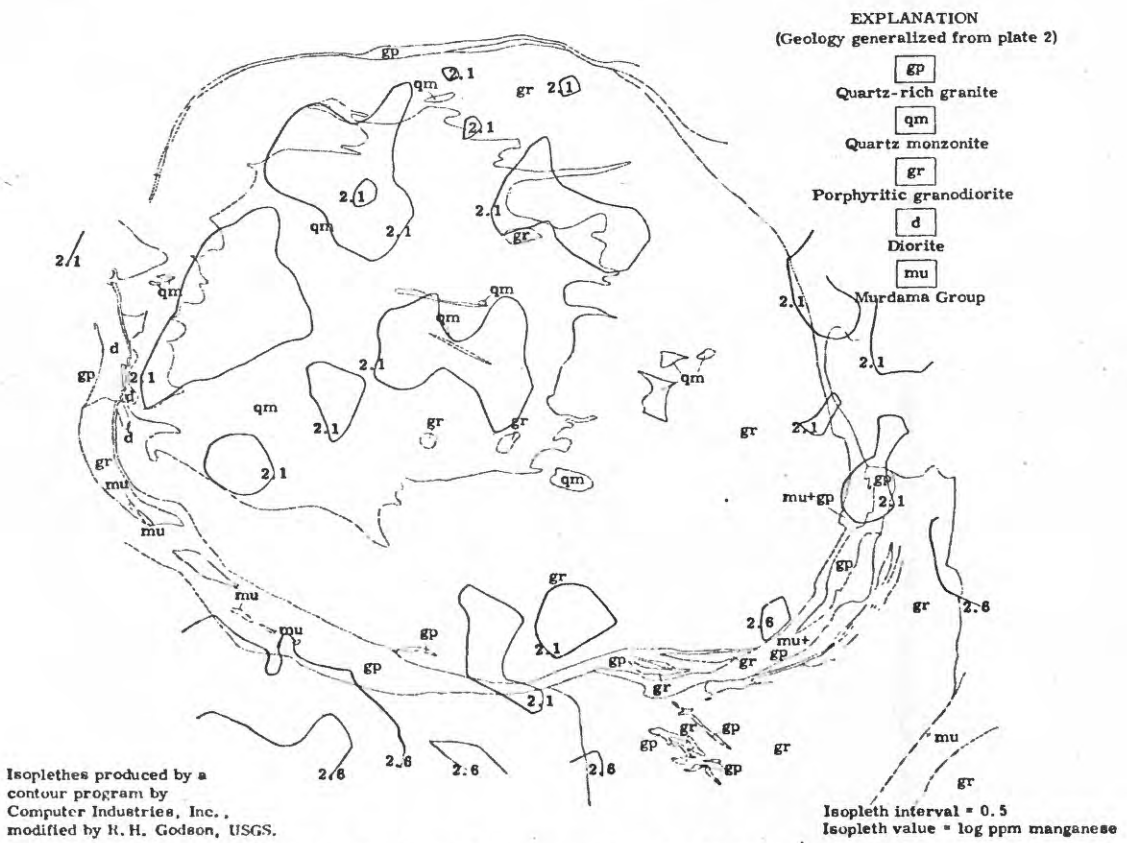

Figure 10.- Distribution of manganese, Uyaijah ring structure.

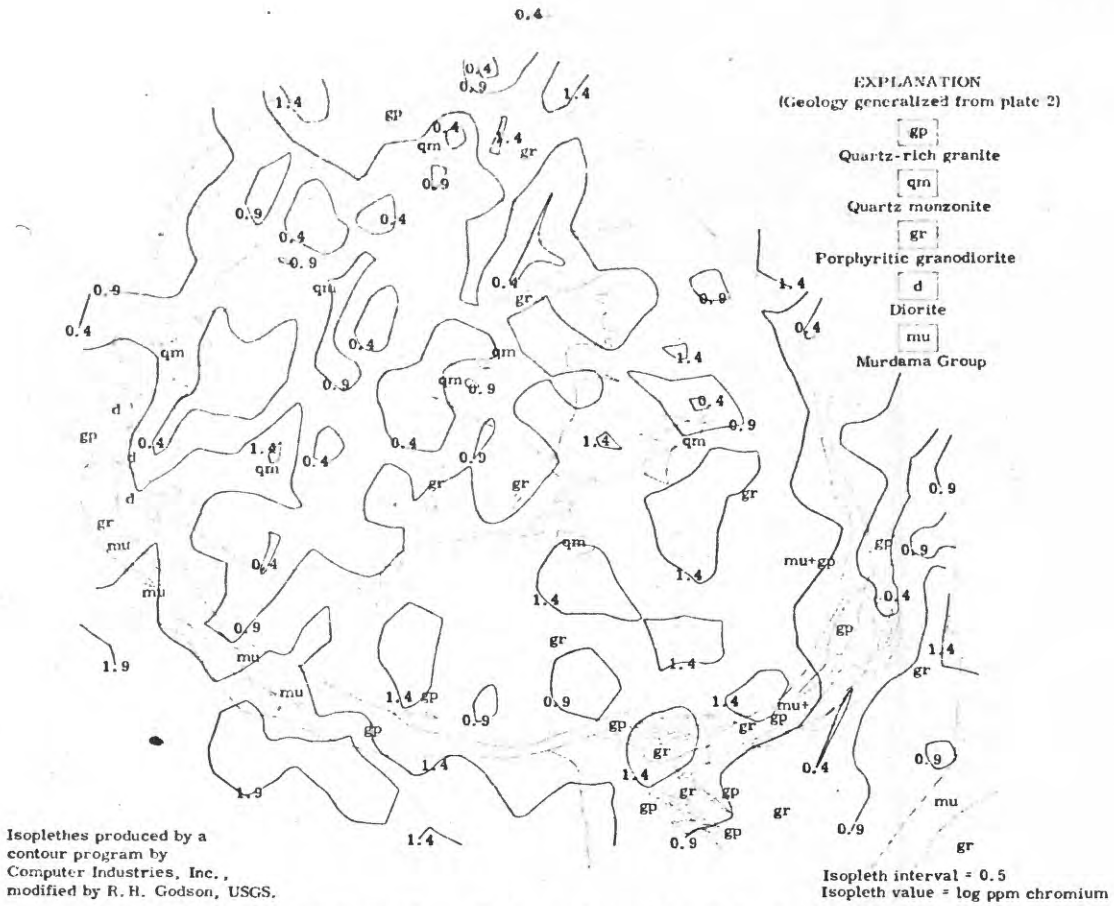

Figure 11.- Distribution of chromium, Uyaijah ring structure.

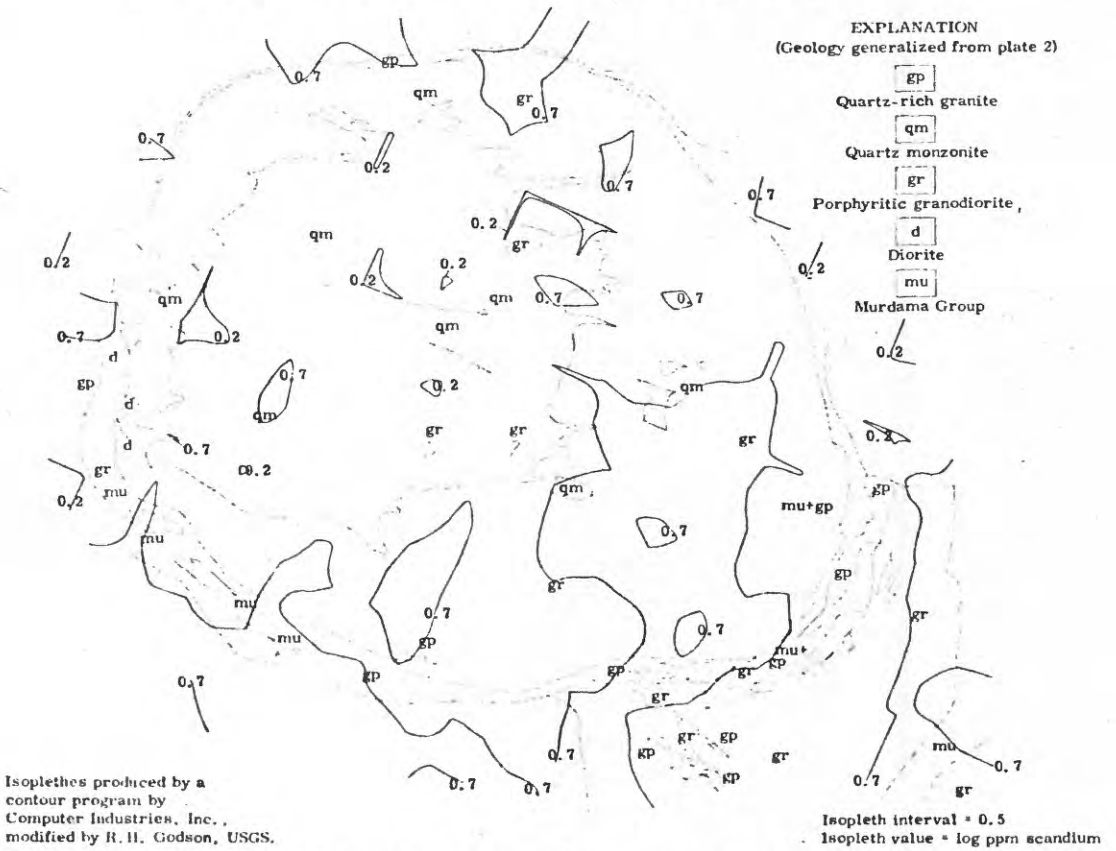

Figure 12.- Distribution of scandium, Uyaijah ring structure.

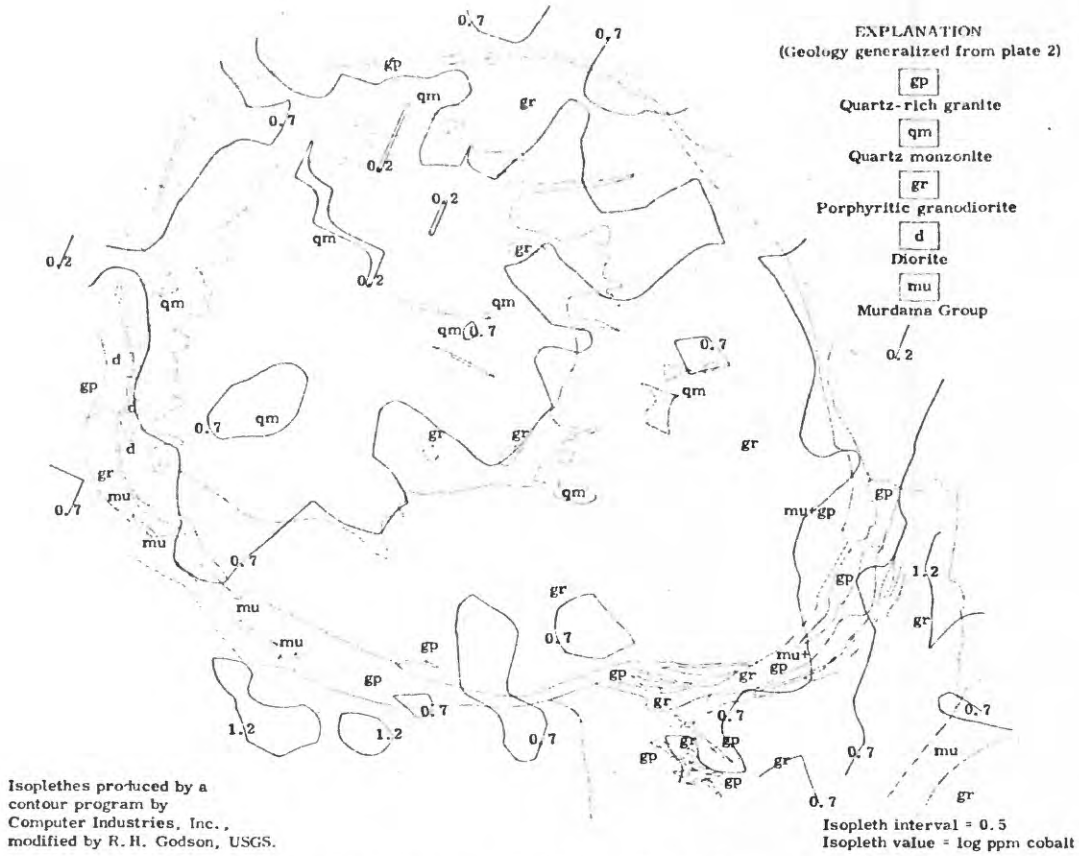

Figure 13. - Distribution of cobalt, Uyaijah ring structure.

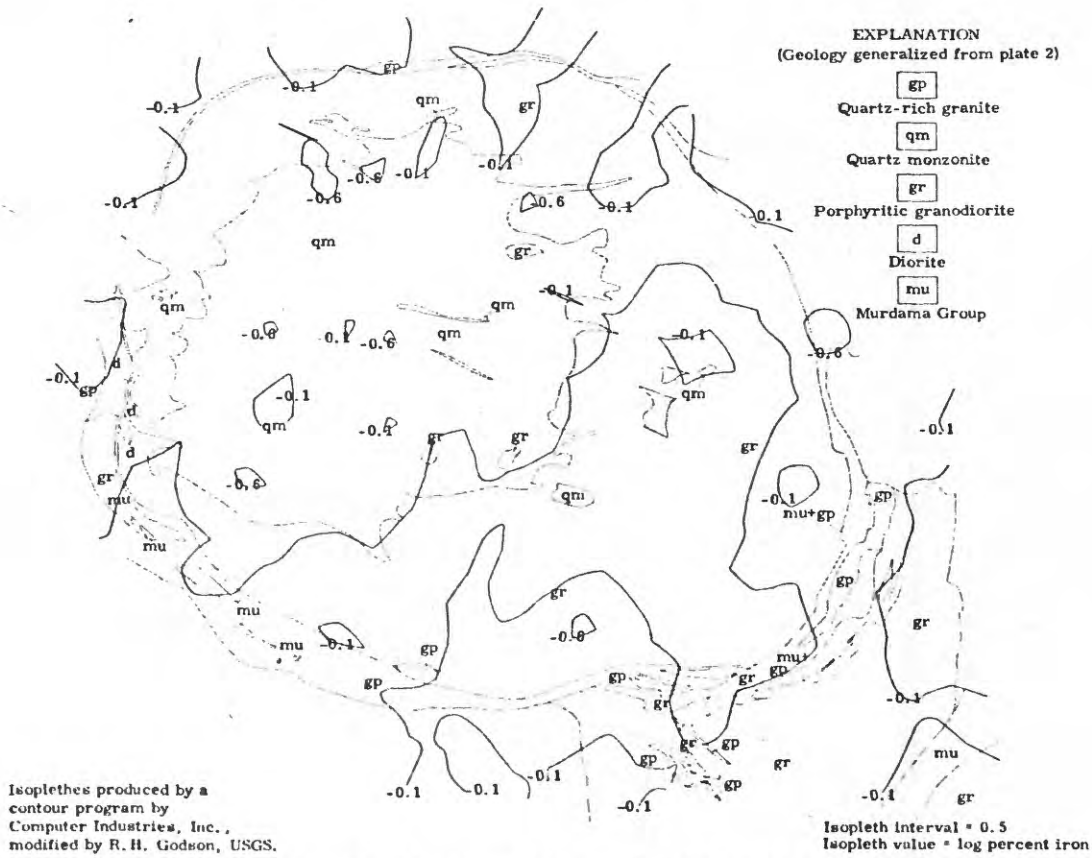

Figure 14. - Distribution of iron, Uyaijah ring structure.

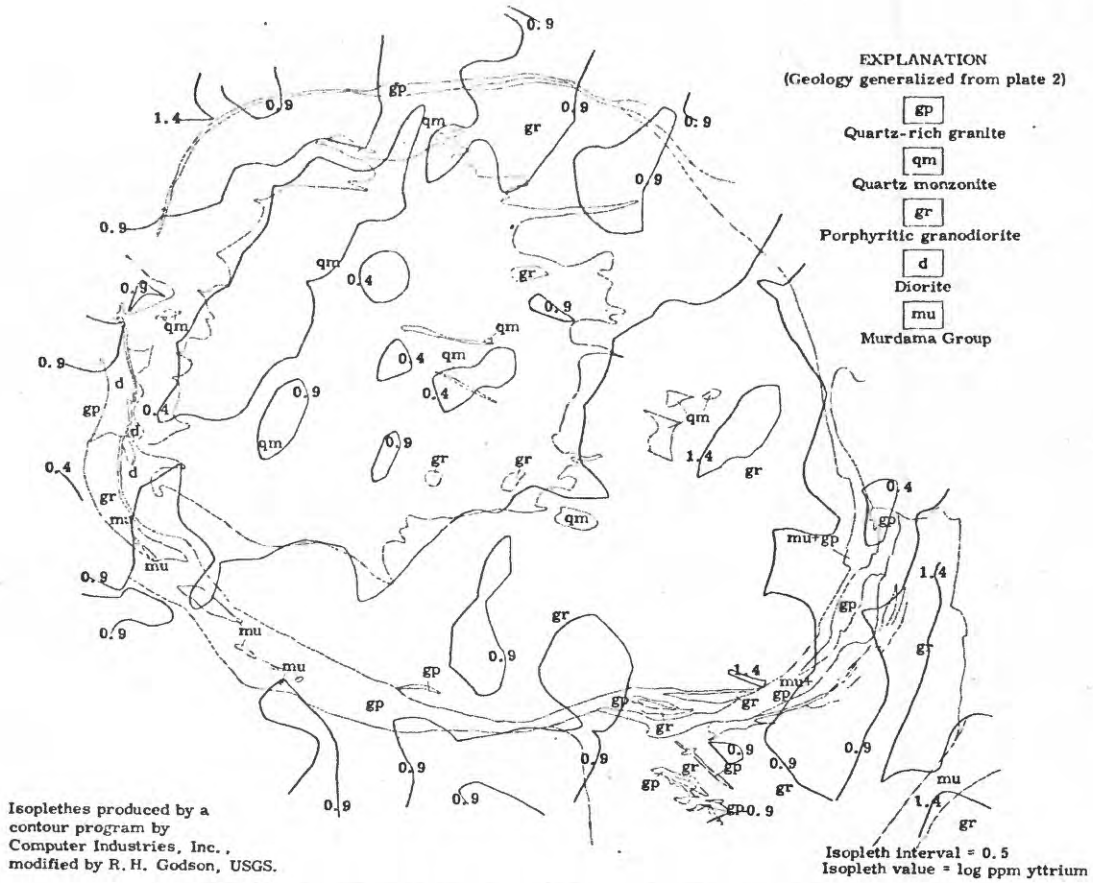

Figure 15. - Distribution of yttrium, Uyaijah ring structure.

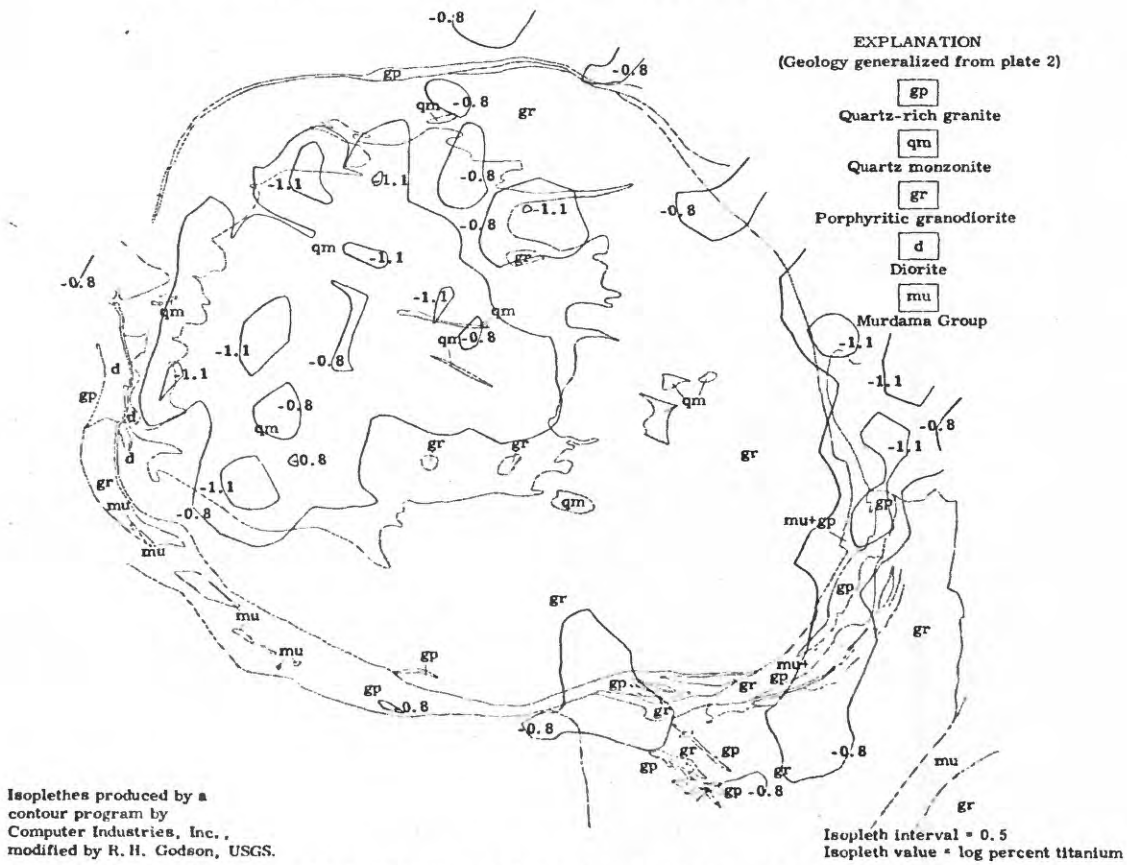

Figure 16. - Distribution of titanium, Uyaijah ring structure.

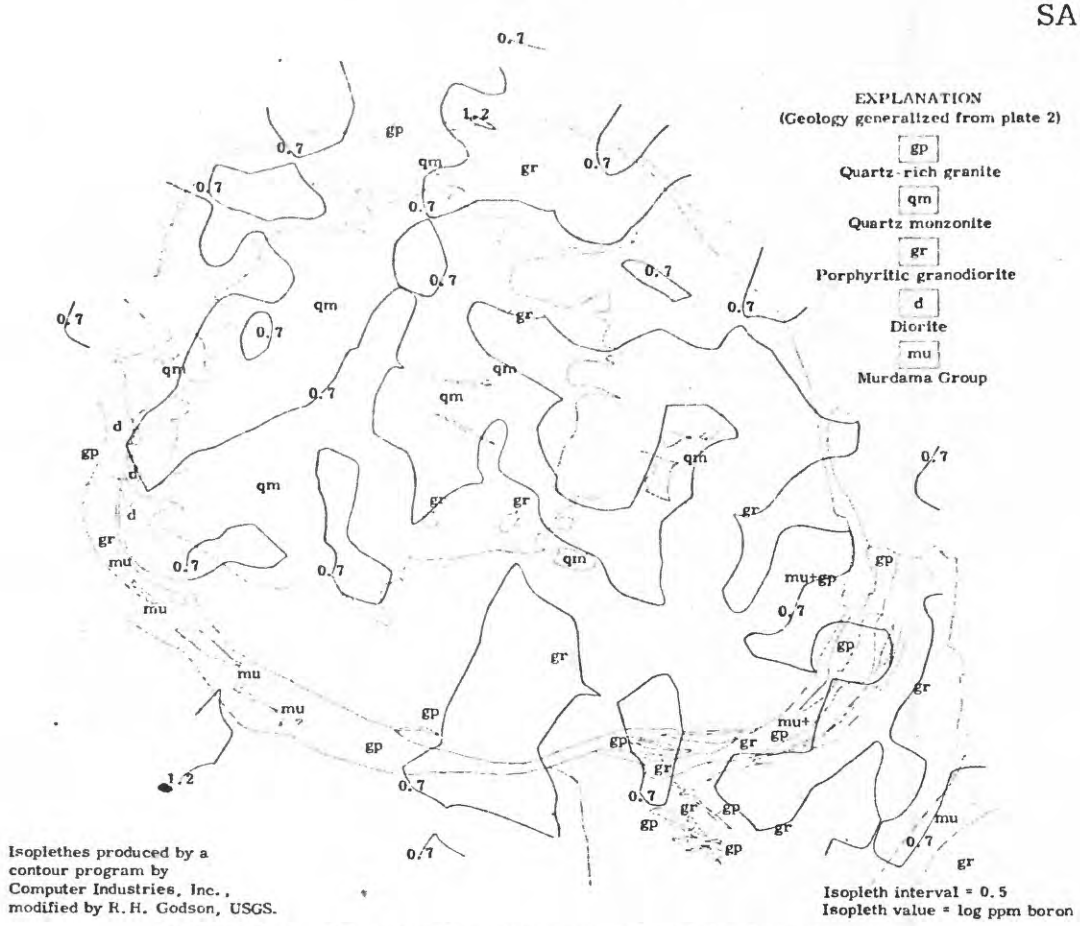

Figure 17. - Distribution of boron, Uyaijah ring structure.

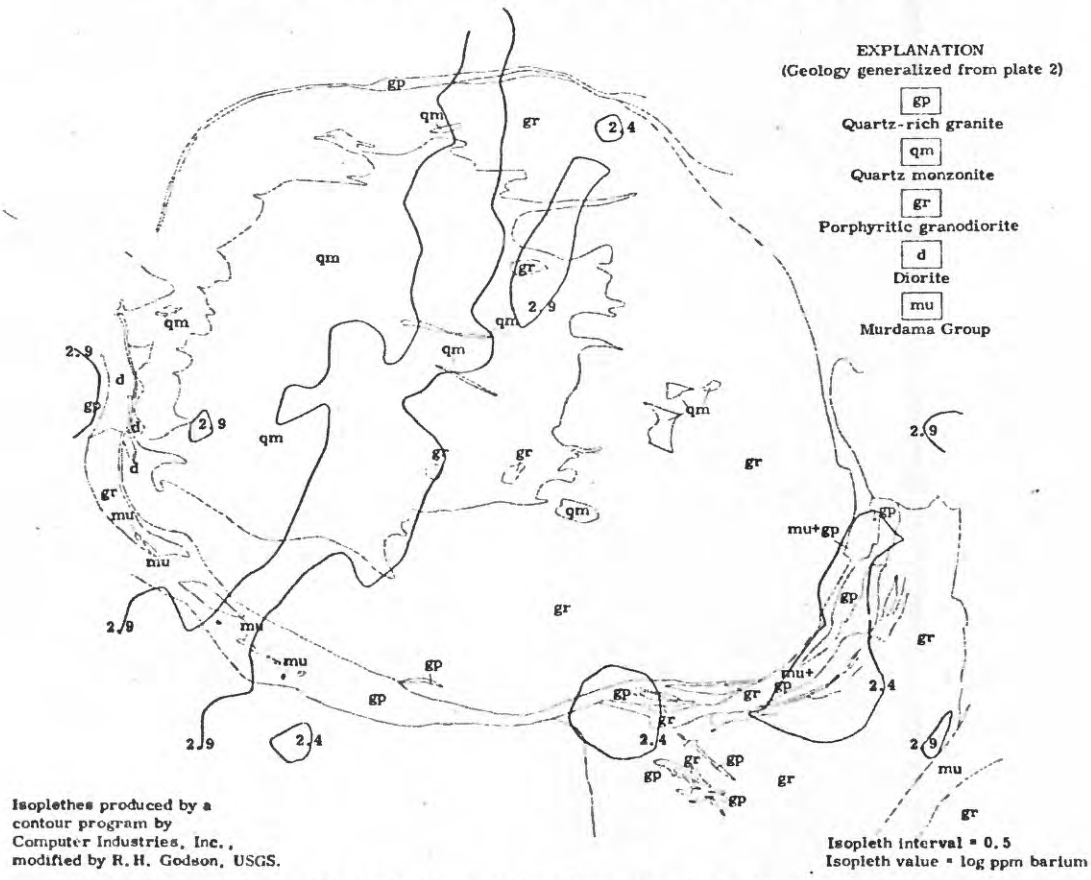

Figure 18. - Distribution of barium, Uyaijah ring structure.

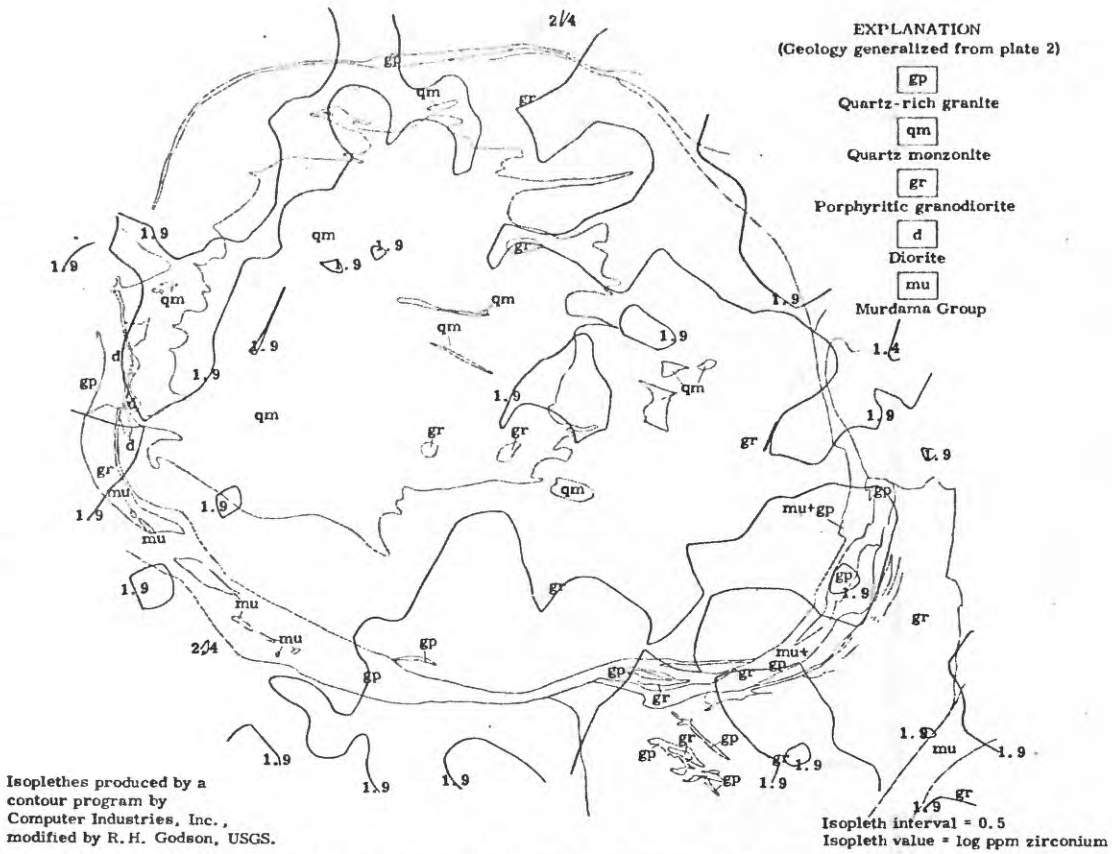

Figure 19. - Distribution of zirconium, Uyaijah ring structure.

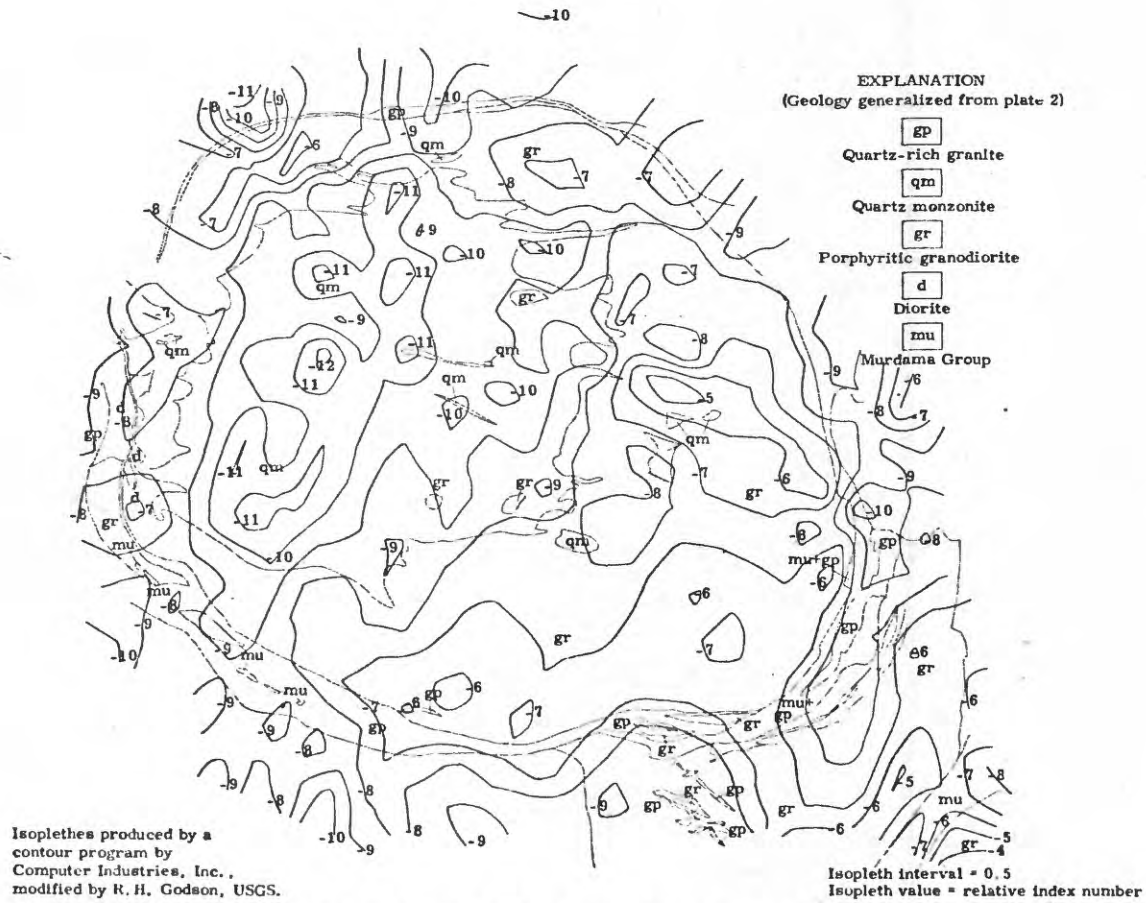

Figure 20. - Granodiorite index map, Uyaijah ring structure.

structure. Those elements with a concentration trend of high, intermediate, and low, respectively, to the Murdama Group of rocks, the porphyritic granodiorite, and the quartz monzonite, are copper, nickel, magnesium, vanadium, calcium, manganese, chromium, scandium, cobalt, and iron. Those elements with a concentration trend of high, intermediate, and low, respectively, to the porphyritic granodiorite, the Murdama, and the quartz monzonite, are yttrium and titanium. Those elements with independent distributive patterns are boron, barium, zirconium, and tungsten.

An index map (fig. 20) of the granodiorite illustrates how the combination of concentrations of elements can be used to emphasize their relationship to the geology. This map was prepared by addition of the effects of titanium and subtraction of the effects of copper and zirconium to the distributive pattern of yttrium.

The elemental distribution maps indicate that distributions of boron, tungsten, barium, and zirconium differ from distributions of the remaining elements in that no trend in concentration is apparently related to the major rock units. The distribution of boron shows a high in the Murdama, no high-low concentration association with porphyritic granodiorite or the quartz monzonite, and an intermediate concentration trending N-S across the central part of the map area. The distribution of barium shows a high trend in the same area as the boron trend and some lows along the southeast portion of the ring that might be associated with the alkaline granite. Tungsten is apparently associated with the alkaline granite but shows an independent pattern relative to the porphyritic granodiorite and the quartz monzonite. Zirconium appears to be acting as a felsic element related to all granitic units.

The trend apparent in the distribution of boron and barium follows the original geochemical orientation line. This line was established to coincide with line 16 of the radiometric survey. The trend, because it follows a line, is suspect but evidence indicates that it may be real. The replicate analyses of some of the samples from this line confirm the trend, and the radiometric survey shows a line-oriented anomaly in this area.

The results of factor analysis of the correlation coefficients of 16 variables, are shown in figure 21. The sixth rotation, which accounts for 85 percent of the variation, is interesting since these six factors can be related to data from other types of analyses. Factor 1 contains copper, nickel, chromium, scandium, cobalt, magnesium, calcium, and iron. The maps showing the areal distribution of these elements (figs. 5-7, 9, 11-14) show a trend of high concentration to low concentration from the Murdama through the porphyritic granodiorite to the quartz monzonite. Factors 2, 3, 4, and 6 are, respectively, barium, tungsten, zirconium, and boron. All of these elements have distributive patterns independent of trends related to the major geologic units. Factor 5 is composed of titanium, yttrium, vanadium, and manganese. The first two of these four elements are the only two which show a trend in distribution from high to low concentration from the porphyritic granodiorite through the Murdama to the quartz monzonite. The presence of vanadium in this factor is supported by other evidence, but manganese is an anomaly in this factor on the basis of present supporting evidence.

A comparison of the results of factor analysis can be made with analyses of fractions of a heavy-mineral suite. A panned concentrate

Variables	Sets of factors from reordered oblique projection matrices.

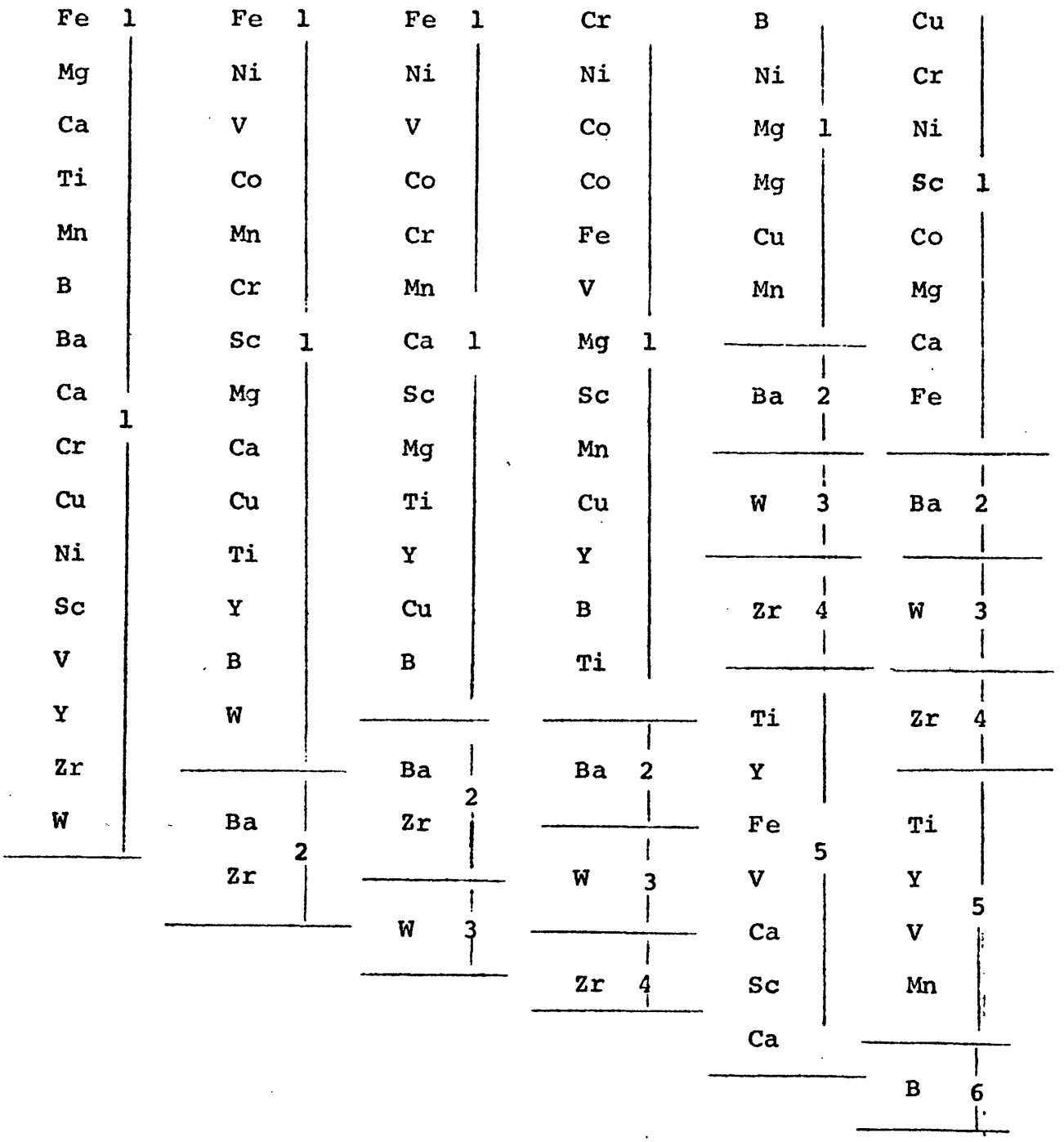

Figure 21. Factors resulting from successive rotations of the 16 variable matrix.

from sample site 60041 was separated into ferromagnetic and nonferromagnetic fractions, and the nonferromagnetic portion was divided into heavy and light fractions with bromoform. The heavy fraction was separated into a number of decreasingly paramagnetic fractions on a Franz Isodynamic separator. These fractions were analyzed spectrographically and concentrations assigned to each element on a scale of 0 to 3, where 0 = not present and 3 = maximum concentration present in the series of fractions. The results of this are plotted in figure 22.

A comparison of the results of factor analysis to the patterns of elemental concentration vs magnetic character shows there is a relationship between the ferride element distributive pattern and the results of factor analysis. Several general patterns (fig. 22) are present in the analysis of the heavy-mineral suite. One is a decreasing concentration with decreasing magnetic character. This pattern is represented by iron, chromium, copper, manganese, calcium, and magnesium. These elements, except for manganese are in factor 1. Another pattern is shown by titanium, vanadium, and yttrium. These elements are in factor 5. A third pattern is increasing concentration with decreasing magnetic character. This pattern is found with zirconium, factor 4. A fourth pattern is found with lanthanum and thorium, which are known to be present in monazite. The pattern of boron is similar in part to that of lanthanum and thorium. Since no tourmaline is reported in these fractions boron may be present in the monazite. In relation to factor analysis the boron distributive pattern in the heavy mineral suite is unique compared to the other elements in the factor analysis matrix and this may contribute to its occurrence as an independent factor. A fifth pattern, that of concentrations of elements detectable only in the most

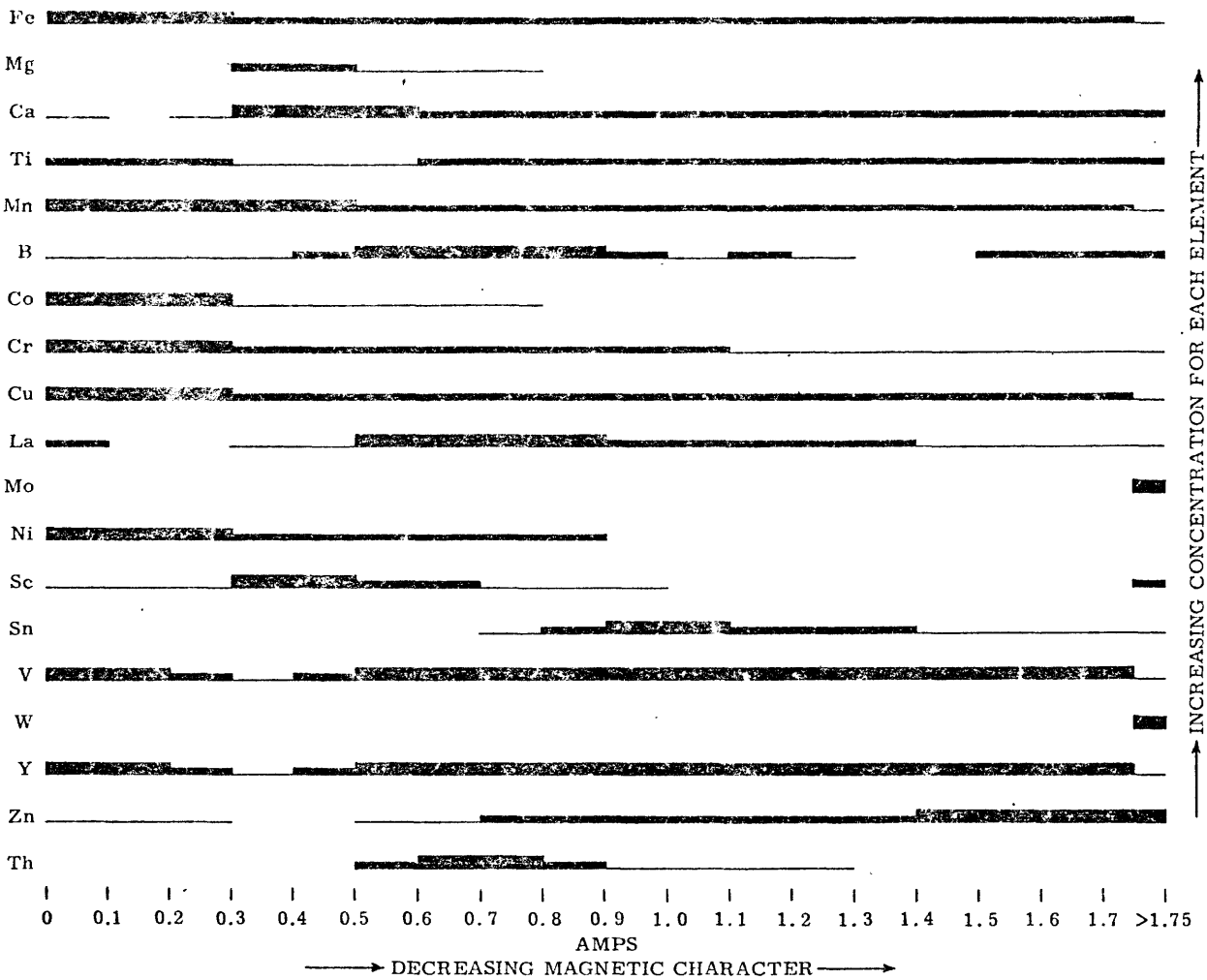

Figure 22.- Plot of variation of magnetic character vs relative concentration of 19 elements in the heavy-mineral suite of sample location 60041.

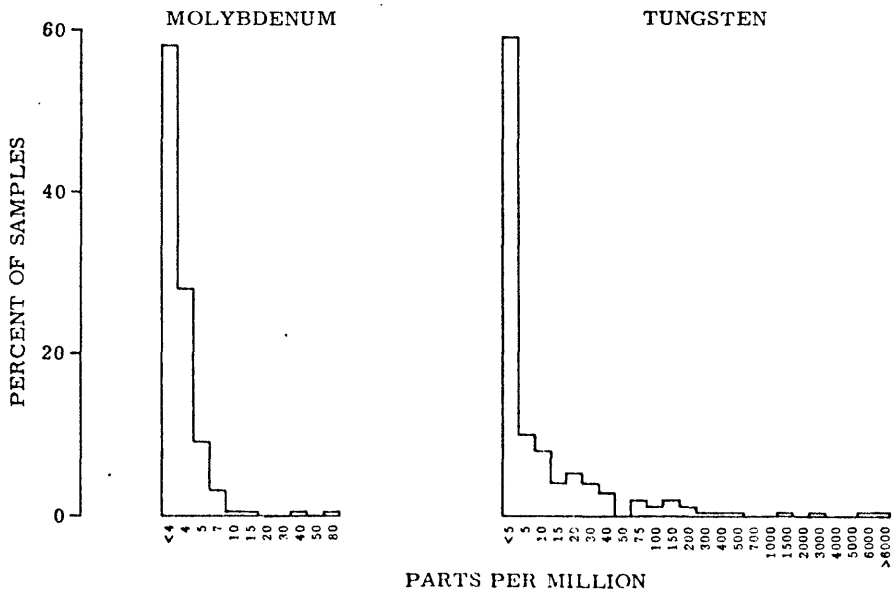

Figure 23.- Tungsten and molybdenum content of heavy-mineral concentrates from the Uyaijah ring structure. Colorimetric analyses by A. A. Redhwi and I. M. Nagvi.

dimagnetic fraction, is shown by tungsten and molybdenum. This is the result of their occurrence in a separate mineral phase which is independent of the ferride elements. This explains the occurrence of tungsten as independent factor 3. The remaining factor, barium, cannot be related to the heavy-mineral suite, because it is not present in detectable quantities. This may explain the presence of barium as an independent factor in a matrix composed essentially of ferride elements.

Evaluation of the maps showing the areal distribution of the elements, the chemical analysis of the heavy-mineral suite, and the factor analysis shows that the variations which are present in the 16 elements can be related to the geologic environment of the Uyaijah ring structure. The ferride elements iron, cobalt, nickel and chromium plus the associated scandium, copper, mangesium, and calcium decrease in concentration from the Murdama through the porphyritic granodiorite to the quartz monzonite. The ferride elements titanium, vanadium, and manganese(?) plus associated yttrium are important constituents in the porphyritic granodiorite where sphene is an abundant accessory mineral. The four elements barium, zirconium, tungsten, and boron each become independent factors. Barium and zirconium are probably associated with the felsic rather than the mafic portion of the samples. Barium may be associated with feldspar, although there is evidence for abundant barium in the ground water and a supergene process may be affecting its distribution. Zirconium is associated with the mineral zircon. Tungsten is found in the mineral scheelite. Boron seems to have a complex distribution. There is evidence for association with the ferride elements, with monazite, with pegmatites, with the vegetation, and with the ground water.

The anomalies

The tungsten content of heavy-mineral concentrates (fig. 23) is the best combination of element and sample medium to define the anomalies. Molybdenum and bismuth in heavy-mineral concentrates supports the anomalies, and lanthanum in heavy-mineral concentrates provides supporting evidence for the interpretation of the anomalies.

The tungsten and molybdenum distributions both have strong positive skewness indicating the presence of an anomalously high group of samples. Surprisingly, the overall distributions for both elements are not strikingly high. The modal values are about normal for the sample medium. The tungsten distribution is sufficiently skewed and covers a sufficient range to allow subdivision of the anomalous data. A simple order-of-magnitude subdivision provides five classes and has been used. The molybdenum distribution is not as readily subdivided, but clearly a single break at 10 ppm will separate the distribution into an anomalous group as opposed to all others. The lanthanum distribution is not represented in the anomalous suite of elements but its distribution in space serves as remarkable supporting evidence for the interpretation of the anomalies. A single break at 1000 ppm lanthanum provides separation of the larger part of the distribution, whose modal value is about 200 ppm, from another group of spacially related samples with high lanthanum content.

Figure 24 shows the distribution of tungsten in respect to the 1 km grid of samples. The data are contoured in the five classes by order of magnitude. Scattered samples or pairs of samples with above average values are occasionally present in the area. Though these samples locally reach into the hundreds of ppm of tungsten, they appear

Figure 24.- Map of the Uyaijah area showing the location of anomalous tungsten, lanthanum, molybdenum and bismuth.

to reflect areas of little immediate economic significance. Three relatively large, more or less continuous highs define the major anomalies and all three reach into the 1000's of ppm. One of these has a pronounced northeast trend across the center of the sample net from near Uyaijah to the vicinity of Jabal Thaaban. This is the anomaly anticipated from the orientation survey. The anomaly is constricted near its midpoint and divided into two parts, the northeastern being the richer by a couple of orders of magnitude. Though this apparent northeast-southwest dicotomy in the anomaly may be real, comparison of figure 24 with the crude physiographic chart of plate 1 suggests that the southwest half of the anomaly could be suppressed by aeolian dilution. This anomaly is in the vicinity of the prominent vein swarms with attendant alteration (fig. 25).

The second and largest anomaly has an arcuate form extending from the west boundary of the data around the southern part of the area and well up the east side of the data, with scattered single highs extending on to the north. Unfortunately this anomaly was not anticipated from the orientation survey; all four legs of the original traverse passed through weak areas of the anomaly. The anomaly was left open at the edge of the data on all sides and additional data had to be collected to the south and east to demonstrate that it did close in an arcuate pattern. The anomaly remains undefined to the west. The anomaly coincides approximately with the outer ring-fracture zone of the Uyaijah ring structure.

The third anomaly is along the east side of the data. It was discovered during the extension of the original sample net, which extension was designed primarily to define the outer-ring anomaly.

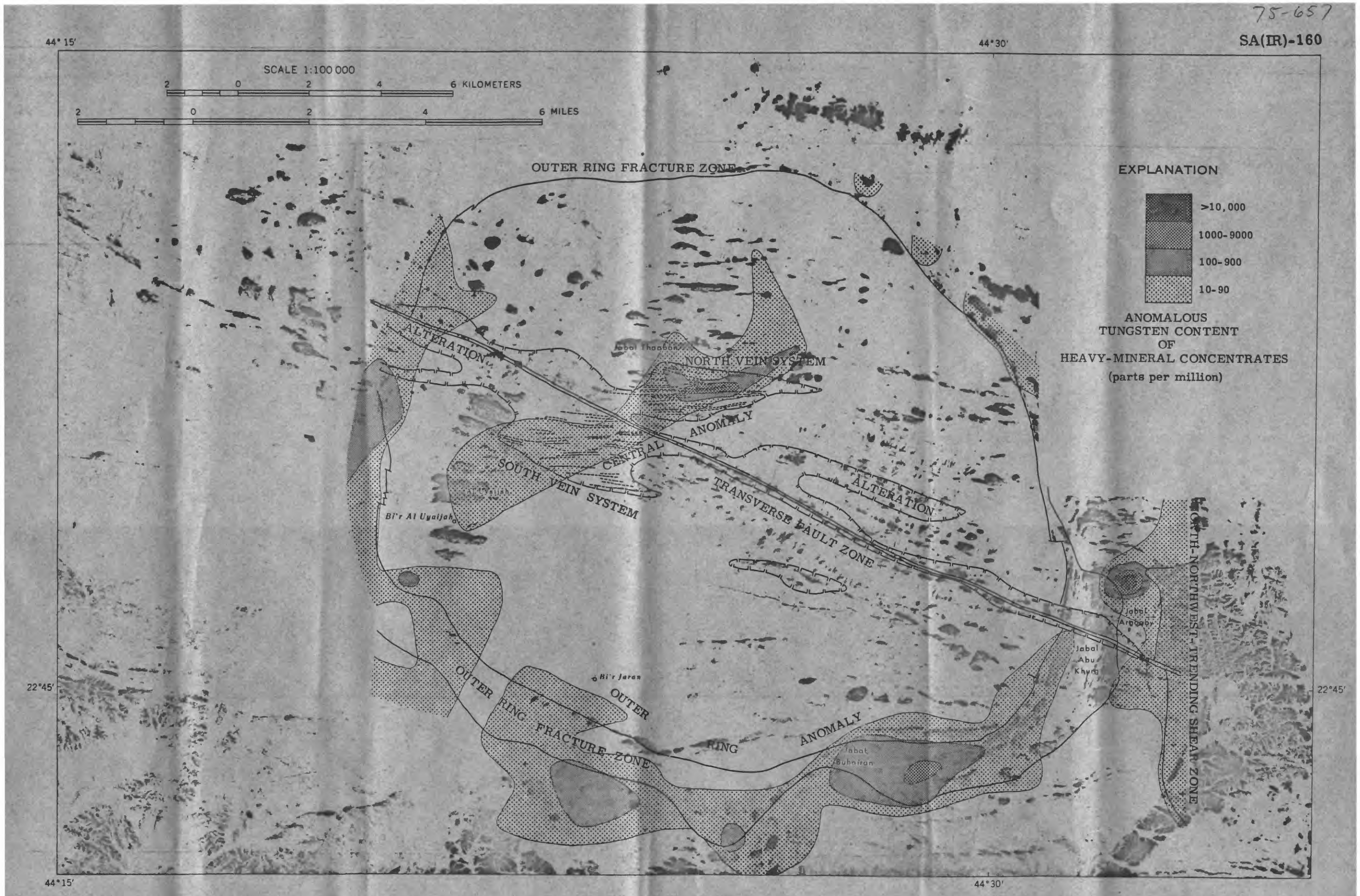

Figure 25. - Selected structural elements of the Uyaijah ring complex in relation to anomalous concentrations of tungsten in heavy-mineral concentrates.

Therefore, the third anomaly remains open to the east. Although the anomaly involves 12 adjacent samples, it is at a generally low level, in 10's of ppm, except for the single sample where overlap with the outer-ring anomaly seems likely. This is the single, most tungsten-rich sample in the matrix. The location of this third anomaly is approximately coincident with the outcrop of sheared rocks along the flank of the north-northwest trending fault to the east of the map area.

The location of samples containing 10 ppm or more of molybdenum is superimposed on the tungsten distribution map (fig. 24). With a single, probably superfluous exception, anomalous molybdenum is in all of the samples containing more than 1000 ppm of tungsten. Molybdenum provides direct confirmation of the tungsten anomaly. The average ratio of tungsten to molybdenum in the concentrates is about 100; the range in individual samples is 50 to 6000. Scheelite from bedrock has a ratio of about 20 and additional molybdenum in molybdenite and pyrite should reduce this figure further. There is evidently considerable loss of molybdenum between the bedrock source and the concentrates analysed here. Evidence for the selective mobilization of molybdenum by a weathering process exists. A relict molybdenum-rich core was observed, using UV-light, in a grain of scheelite, indicating a selective dissolution of molybdenum during weathering since crystals of scheelite observed in place are uniformly colored yellowish. Analyses of ground water from two wells in the area indicate that considerable molybdenum is present in the ground water. Water from Bi'r Gairan, in an apparently unmineralized area, contains 100 ppm of molybdenum, while water from Bi'r Uyaijah, in a silicified, mineralized area contains

400 ppm molybdenum. The bedrock anomaly should be considerably richer in molybdenum and at least somewhat richer in tungsten than the anomalies we have obtained in the transported material.

Bismuth was detected spectrographically at the 10 ppm limit of sensitivity in heavy-mineral concentrates numbered 3, 181, and 41 in the central anomaly and 252 and 377 in the outer-ring anomaly. The presence of bismuth provides additional confirmation for the anomalies. The bismuth reported in samples 181 and 377 is sufficiently high, 200 ppm, to suggest the possibility of a separate mineral phase and to draw more attention to this element. Interference by the abundance of iron and, particularly, titanium in the concentrates hindered spectrographic determination of bismuth. Therefore colorimetric analyses of selected samples for bismuth was used for confirmation. The additional analyses suggest even higher values may be present: as much as 1000 ppm. If further analyses confirm presence of bismuth at this level then bismuth becomes a major component of the anomaly.

The lanthanum distribution in heavy-mineral concentrates is also superimposed on the tungsten distribution in figure 24. A single threshold value of 1000 ppm has been shown to define only the highs. Normal background in the surrounding terrane, underlain by the calc-alkaline granitic rocks, is of the order of 200 ppm or less. The general coincidence of the enrichment in lanthanum with the tungsten anomalies, particularly the coincidence with the central anomaly, lends strong support to our hypothesis of association of the anomalies with rocks of the alkaline granite series. The association is particularly useful in the central anomaly where the presence of a buried cupola of alkaline granite can only be inferred.

The main tungsten anomalies are superimposed on selected features of the geology in figure 25. The anomalies are clearly related to the two vein swarms, the ring-fracture zone, and the north-northeast-trending shearing. There is no evidence for a relationship between the anomalies and the transverse-fault zone. The maximum amplitude of the anomalies is reached in the central anomaly and in the southeastern part of the outer ring anomaly.

These anomalies are interpreted to result from leakage of tungsten and molybdenum from the upper parts of an alkaline granite stock. The tungsten-bearing volatiles have escaped along the sheared rocks of the ring-fracture zone and through the shattered rocks over the inferred cupola in the central part of the structure. Minor additional leakage into sheared rocks adjacent to the north-northwest-trending fault may be facilitated by constriction of the ring fracture zone by the east lobe of quartz monzonite, leading to a local peak concentration of metal where the ring fracture abutts the quartz monzonite. Accepting this interpretation, we have a preference for the central anomaly as the one with the greatest potential to have accumulated the greatest amount of metal in the smallest area. In any event it is clear that the central anomaly and the outer ring anomaly are separate entities, emplaced in different tectonic settings. They should be evaluated as different anomalies.

Sample 193 at the south edge of the ring structure contains 700 ppm lead, 700 ppm zinc, and detectable silver in the surficial debris. Search of the area to the south of this sample locality during later sampling revealed the presence of filled trenches and building foundations from an ancient mining venture. Analyses by S. U. Qubai of a

composite grab sample of carbonate, quartz, and breccia vein material from spoilage piles adjacent to the trenches yielded 2.3 oz/ton silver, 2.5 percent zinc, and 0.65 percent lead, with a trace of copper and gold.

SUMMARY AND RECOMMENDATION

The Uyaijah ring structure appears from present information to be the most favorable site for tungsten-bismuth-molybdenum mineralization in the Kushaymiyah area. The geochemical anomalies that have been developed in the area to date have two geologic settings. Although these settings are probably part of a single genetic system, they can be expected to have different physical characteristics. As interpreted here, the genetic link between the two settings is the alkaline-granite suite of rocks. These are related in space and time to both the outer-ring anomaly, presumably the result of leakage from a deeper alkaline-granite mass along the ring fracture that permitted intrusion, and to the central anomaly, presumably the leakage above a cupola in the underlying alkaline granite. In the outer-ring anomaly, tungsten, molybdenum, and presumably bismuth minerals are found in the regular, arcuate fracture system that bounded the structure. The most intense mineralization appears to be around the southeast quadrant of the structure. In the central anomaly, minerals of the same elements are found associated with swarms of massive quartz veins in a more diffuse, discontinuous set of east-trending fractures.

Definition of the anomalies is much more clear - they have been fairly well defined both geographically and geologically. However, the present work based on a 1 km grid, must be considered as reconnaissance. In order to define specific mineralized targets the two types

of anomaly should be studied in much more detail both geologically and chemically. Toward this end, two smaller areas within the Uyaijah ring structure have been recommended for study at a scale of 1:10,000. The northern of these (pl. 1) is 3.5 km wide and 11 km long, extending in a northeasterly direction along the central anomaly from near Bi'r al Uyaijah to and beyond Jabal Thaaban. This might best be referred to as the Uyaijah-Thaaban area. The southern area is 3 km wide and 12 km long, extending in a dog-legged fashion from the vicinity of Jabal Buhairan to and beyond Jabal Abu Khurg. This might best be referred to as the Buhairan-Abu Khurg area.

Each of these areas is of the order of 35 to 40 sq km. At a scale of 1:10,000, each constitutes a project in itself. Sampling on about a 100 m grid would require 3500 to 4000 samples for each area, with geologic detail to match. This spacing is still sufficiently open that heavy-mineral concentrates probably remain the most suitable medium for definition of the anomalies. Hopefully, surficial debris without concentration would begin to define variations within the data, but this point cannot be demonstrated. The value of rock sampling for regional variations continues to be slight because the metals of interest are evidently in discrete, concentrated mineral phases. Although anomalous rock samples would probably be obtained on a 100 m grid, the variations would probably be extremely erratic. The principal metals of interest are tungsten, molybdenum, and bismuth.

We feel that the work to date is sufficiently encouraging to justify proceeding to the next step. Progress beyond that step will depend upon its outcome. Should the area continue to be promising from the detailed studies, other parts of the Kushaymiyah complex outside

of the Uyaijah ring structure should be re-evaluated, particularly a similar appearing ring structure to the north.

LITERATURE CITED

Bois, J., and Shanti, M., 1970, Mineral resources and geology of the As Sakhan quadrangle, photomosaic sheet 130; French Bur. Recherches Géol. Minières open-file rept. 70-6.

Eijkelboom, G., 1966, The mineral resources and geology of the Idsas - Wadi Jifr region (sheet 117, Zone 2): French Bur. Recherches Géol. Minières open-file rept. 66-A-15, 38 p.

Flanigan, F. J., 1967, U. S. Geological Survey silicate rock standards: Geochem. et Cosmochim. Acta, v. 31, p. 289-308.

Fleischer, M., 1965, Summary of new data on rock samples G-1 and W-1, 1962-1965: Geochim. et Cosmochim. Acta, v. 29, p. 1263-1283.

Jackson, R. O., Bogue, R. G., Brown, G. F., and Gierhart, R. D., 1963, Geologic map of the Southern Najd quadrangle, Kingdom of Saudi Arabia: U. S. Geol. Survey Misc. Geol. Inv. Map I-211A.

Leca, X., 1970, Mineral resources and geology of the Jabal Sahah quadrangle, photomosaic sheet 132 east: French Bur. Recherches Géol. Minières open-file rept. 70-7, 27 p.

Theobald, P. K., 1971, Al Kushaymiyah as a target for a Colorado-type molybdenite deposit, Southern Najd quadrangle, Kingdom of Saudi Arabia: U. S. Geol.Survey open-file report (IR)SA-120, 13 p., 3 plates, 2 figs.

Vincent, G., 1968, Geology and mineral resources of the Halaban-Sabhah region (sheet 118 - Zone 2): French Bur. Recherches Géol. Minières open-file rept. 68-1, 47 p.

Whitlow, J. W., 1966a, Geology and geochemical reconnaissance of the Jabal al Hawshah quadrangle, Southern Najd: Saudi Arabian Dir. Gen. Mineral Resources Mineral Investigations Map MI-16.

Whitlow, J. W., 1966b, Geology and geochemical reconnaissance of the Al Kushaymiyah quadrangle, Southern Najd: Saudi Arabian Dir. Gen. Mineral Resources Mineral Investigations Map MI-17.

Whitlow, J. W., 1971, Areas in the Southern Najd quadrangle, Saudi Arabia, recommended for mineral investigations: U. S. Geol. Survey open file report (IR)SA-79, 11 p., 2 figs.

SECTION B

REGIONAL GEOPHYSICS

by

Vincent J. Flanigan and Gordon E. Andreasen

INTRODUCTION

A geophysical study, including an airborne gamma-radiation survey in four areas covering about 2500 sq km, and aeromagnetic interpretation, was made in the Kushaymiyah area (fig. 1) in support of the geological and geochemical investigations described in Section A. Integrated geophysical study using both techniques is particularly helpful, because the two techniques often compliment each other. Geologic units which show no marked magnetic features may be distinguished by their radiation. Likewise, structural features, and geologic units of similar chemical composition, which have no characteristic radiation patterns can often be delineated by their magnetic response.

GAMMA RADIATION

The radiation data is presented as contour maps (fig. 26) of total count, plus isoelement maps (figs. 27-29) of potassium (K^{40}), thorium (as Ti^{208}), and uranium (as Bi^{214}), the three elements largely responsible for naturally occuring terrestrial gamma radiation.

Flight line spacing of 1 km and flight height of 91.5 m were selected to yield reconnaissance data over the area flown. At the line spacing selected, the crystal detectors would not provide data with line to line overlap, because the detectors record little or no contribution from radiation sources beyond 150 m in a horizontal direction normal to the line of flight. Radiation features of sufficient size to be mapped at 1:100,000 scale would, however, show a response on adjacent lines.

There are indications that mineral concentrations are related to areas of higher radiation response. These relationships might be more firmly established by analysis of data from a detailed airborne survey. The outstanding feature from the present investigation is the correlation

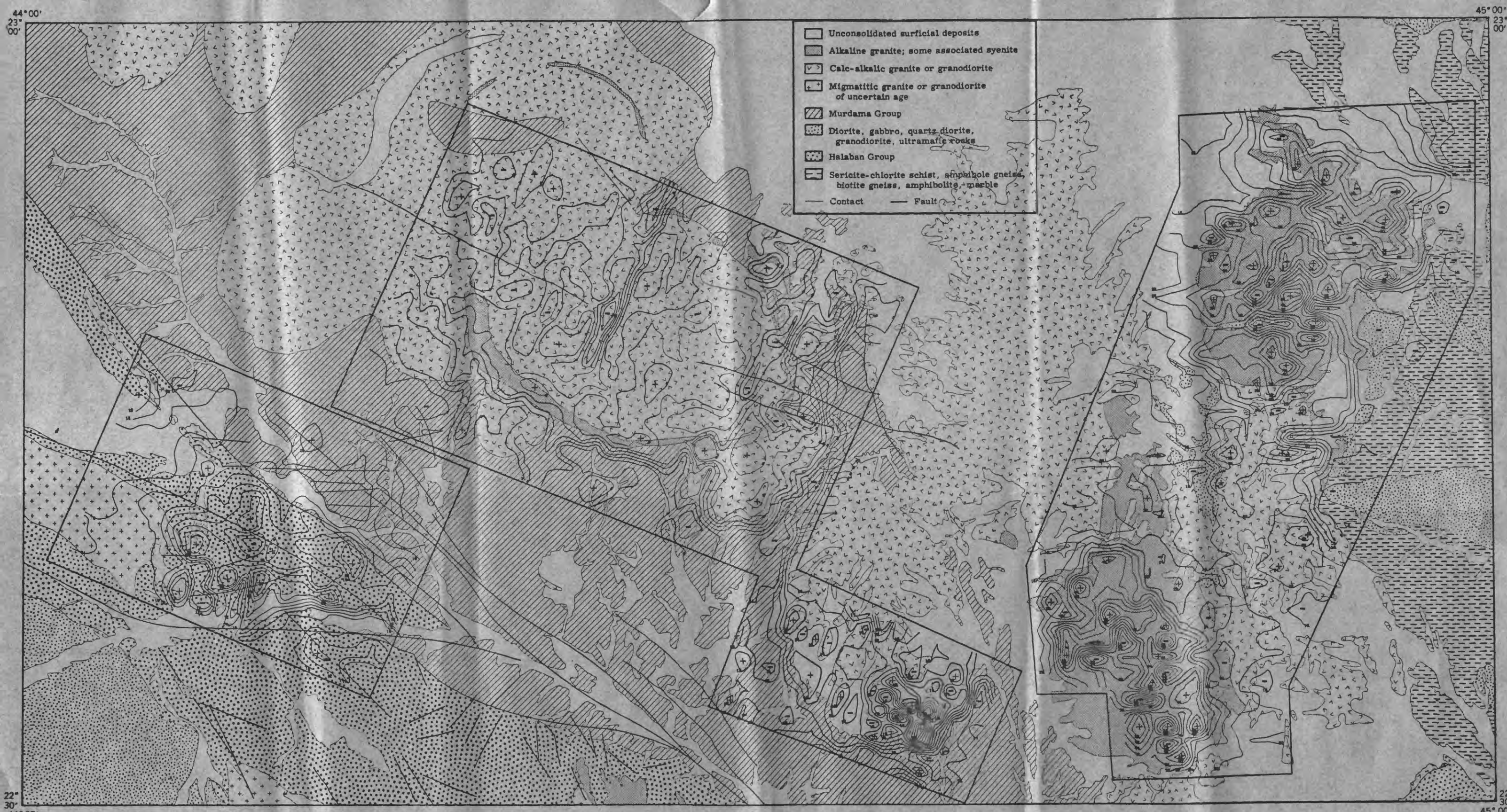

Airborne gamma radiation survey and compilation by U.S. Geological Survey Saudi Arabian Project, 1971. Geology generalized from unpublished (1971) maps by French Bur. Recherches Geol. Minieres.

SCALE 1:250 000

5 0 5 10 15 KILOMETERS

5 0 5 10 15 MILES

Radiometric contour
Contour interval: 1000 counts per minute
Radiometric high + Radiometric low −
Mean flight spacing: 1 km
Mean terrain clearance: 91.5 m (300 ft)

Figure 26. - Generalized geologic map of the Kushaymiyah area showing isoradiometric contours (total count).

75-657

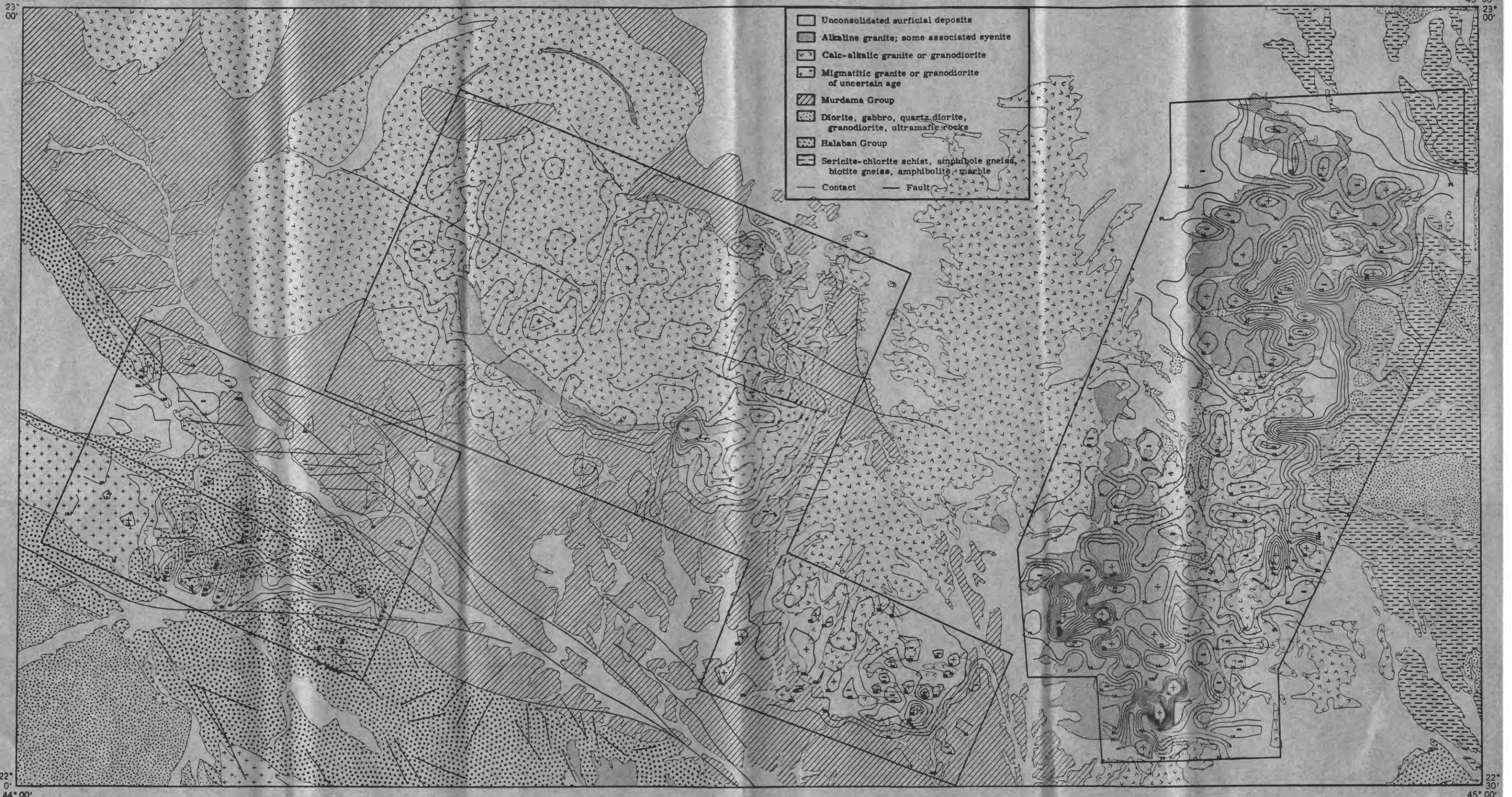

Airborne gamma radiation survey and compilation by U.S. Geological Survey Saudi Arabian Project, 1971. Geology generalized from unpublished (1971) maps by French Bur. Recherches Geol. Minieres.

SCALE 1:250 000

5 0 5 10 15 KILOMETERS

5 0 5 10 15 MILES

Radiometric contour
Contour interval: 100 counts per minute
Radiometric high + Radiometric low –
Mean flight spacing: 1 km
Mean terrain clearance: 91.5 m (300 ft)

Figure 27. - Generalized geologic map of the Kushaymiyah area showing isoradiometric contours (uranium).

Airborne gamma radiation survey and compilation by U.S. Geological Survey Saudi Arabian Project, 1971. Geology generalized from unpublished (1971) maps by French Bur. Recherches Geol. Minieres.

Figure 28.- Generalized geologic map of the Kushaymiyah area showing isoradiometric contours (thorium).

75-657

44°00′
23°
00′

45°00′
23°
00′

Unconsolidated surficial deposits
Alkaline granite; some associated syenite
Calc-alkalic granite or granodiorite
Migmatitic granite or granodiorite of uncertain age
Murdama Group
Diorite, gabbro, quartz diorite, granodiorite, ultramafic rocks
Halaban Group
Sericite-chlorite schist, amphibole gneiss, biotite gneiss, amphibolite, marble
Contact
Fault

22°
30′
44°00′

22°
30′
45°00′

Airborne gamma radiation survey and compilation by U.S. Geological Survey Saudi Arabian Project, 1971. Geology generalized from unpublished (1971) maps by French Bur. Recherches Geol. Minieres.

SCALE 1:250 000

5 0 5 10 15 KILOMETERS

5 0 5 10 15 MILES

Radiometric contour
Contour interval: 100 counts per minute
Radiometric high + Radiometric low −
Mean flight spacing: 1 km
Mean terrain clearance: 91.5 m (300 ft)

Figure 29.- Generalized geologic map of the Kushaymiyah area showing isoradiometric contours (potassium).

of the radiation patterns with the mapped geology. This observation suggests the usefulness of gamma radiation as an aid to regional geologic mapping.

Survey instrumentation and procedures

The gamma spectrometer measures and records on separate channels gamma radiation emitting from potassium, thorium, and uranium, as well as total radiation response at a selected sampling rate along a flight line. Normal flight height is about 100 m above the ground. Actual flight height is measured by a radar type altimeter and is recorded at the same rate as the other channels. The five channels of information are recorded simultaneously on an analog strip chart and on computer compatible magnetic tape. Events occurring along the flight path are timed by a master digital clock in the incremental digital tape recorder. The flight path is recovered from observed documentation points and strip film from a 35 mm tracking camera. The ground to air calibration of the equipment was not complete at the time, so all measurements are relative and cannot be related directly to absolute values of mineral concentration on the ground.

Data reduction

Data recorded on magnetic tape is processed by automatic data processing methods on an IBM 360/50 computer at the College of Petroleum and Minerals Computer Center, Dhahran. Computer programs in use have been developed or adapted by the USGS/SAG project for this particular application and equipment.

The data is processed by application of several procedures. The raw data is adjusted by a sensitivity conversion to counts per minute, then a base adjustment is made to correct for the contribution of cosmic

radiation. An altitude correction is applied to the data and the potassium and uranium channels receive a correction which nulls the interelement response relationship. The data is digitally filtered to remove high frequency noise from the signal. Amplitude ratios are computed between the three primary channels and all data channels are merged with flight line documentation and an x-y position is computed for each data observation. The flight line data is gridded by a program which interpolates and assigns a data value to each intersection of the selected grid lines. The resultant data is then automatically contoured on an EAI model 430 Dataplotter. Profiles of processed flight line data and ratio maps of potassium, thorium, and uranium are on file for future use, but because of the added volume of data are not included in this report.

Area 1

The radiation data for area 1 (figs. 26-29) shows a moderate to good radiation contrast between metasedimentary rocks mapped as the Murdama Group and adjacent granitic rocks at the southern and eastern edges of the surveyed area. The contact between these rocks is characterized by steep radiometric gradients which can be seen most easily on the total count and uranium maps and to a lesser degree on the thorium map. This is consistent with the expected higher contents of uranium and thorium in granites. In the south-central part of the surveyed area there is a body of granite shown on the geologic map that has no marked radiation gradient between it and the Murdama. This inconsistancy suggested an error in previous geologic mapping which was confirmed by detailed inspection (Paul Theobald, personal comm.) on the ground.

The Uyaijah ring structure exhibits the highest radiometric expression. This is typical of the late stage alkaline granitic intrusives mapped on the Arabian Shield. The Uyaijah ring structure is well defined on the east by a series of coalescing anomalies for uranium and thorium. On the south the radiometric expression of the Uyaijah ring is considerably less and tapers off to the east, with only a suggestion that there may be a surface expression of the ring structure in the northwest quadrant of the surveyed area.

In the center of the surveyed area there are two low-amplitude radiometric highs for thorium and uranium that trend northeast. These highs are nearly coincident geochemical anomalies and possibly reflect an increased radiation response from two swarms of quartz veins that may be associated with the geochemical anomalies. The two radiometric highs are separated by a pronounced low most clearly seen on the total count map, but reflected on the thorium and uranium maps. Inasmuch as the trend of the low parallels the flight-line direction the data were suspect at this point as being possibly incorrect. However, it has been suggested that this low may reflect a local increase in the thickness of aeolian sand surficial overburden, an interpretation partly borne out by a geochemical low in the same area (Theobald, 1971, personal commun.).

In general, the radiation responses of the uranium and thorium channels are the most definitive. Changes in potassium channel are more subtle. There is lower potassium response (fig. 29) from the Murdama than from the granitic rocks, and the alkaline granite displays a somewhat higher potassium response than the other granites. Local variations of potas-

sium within the granite body enclosed by the Uyaijah ring structure cannot be related to known physiographic or geologic features; interpretations would require additional knowledge of the potassium chemistry.

Variations in type and depth of surficial cover and local variations in weathering and leaching, which contribute to changes of isoelement concentration, are among some of the possible explanations for changes in radiation response that cannot be related directly to changes in lithology. In addition, local highs may reflect deviation from the normal in those areas where the low-flying aircraft passed close to a radiation-contributing isolated granite mass rising prominently above the pediment surface.

Area 2

Metasedimentary and metavolcanic rocks of the Murdama and Halaban Groups, and a mass of granite and granodiorite, are the principal rocks in area 2, which are transgressed by northwest-trending major faults of the Najd Fault system. A thick cover of aeolian sand obscures the radiometric reflection of the bedrock over much of area 2.

The maps showing isoelement radiation (figs. 27-29) disclose comparatively high radiation over the Halaban Group, which serves to distinguish these rocks from the Murdama on the northern contact and granite and aeolian sand to the east. The extent of the aeolian sand can be seen particularly well on the potassium map (fig. 29), where the sand accounts for a radiation low. Another potassium low in the southwest quadrant of area 2 also may be attributed to aeolian sand. Local radiation highs within the Halaban, reflected on all the isoelement maps, may be partially attributed to pegmatite dikes shown on BRGM maps as pegmatite with uranium. Several localities with pegmatite dikes

correlate well with local radiation highs, from which it is inferred that other radiometric highs in this area may reflect unmapped pegmatites.

Area 3

Area 3 is occupied by bodies of alkaline granite separated by a calc-alkaline granite mass. Diorite and amphibole gneiss crop out on the east and northeast edge of area 3. The south lobe of alkaline granite forms Jabal Al Hawshaw, and the north lobe underlies Jabal Hawshat Ibn Huwayl.

The uranium and thorium isoelement maps (figs. 27-28) outline the granite bodies particularly well by reflecting increased radiation response characterized by coalescing highs, and by sharply defined contacts as seen by steep radiation gradients. There is, however, one area on Jabal Al Hawshah where the radiation pattern is not consistent with the mapped geology, which shows a lobe of alkaline granite extending northward from the main granitic mass. Additional data on the rocks in the area would be required to explain the difference between the radiation response and the mapped geology.

The contact between the granite bodies and the diorite and gneiss to the east and northeast is clearly defined by steep radiation gradients and can be traced on all the radiation maps. The two prominent deviations in contours which depart from the mapped geologic contact remain unexplained at this time.

The radiation response over Jabal Hawshat Ibn Huwayl, the northernmost of the alkaline granites, shows a series of lows near the center of the mass. These lows are most clearly seen on the total count map but are reflected to some extent on each of the isoelement maps, and most likely reflect the heterogeneous character of the granite. Both

lobes of alkaline granite exhibit local radiometric highs which are roughly coincident on all the isoelement maps, indicating areas of mineral concentration that give rise to increased radiation response. This is the typical radiation response of the alkaline granite and probably is of no economic interest.

Area 4

Murdama rocks and a mass of calc-alkaline granite are the lithologic units in area 4. The flat pediment surface of area 4 is broken by several inselbergs of granite. The pediment is covered with a thin veneer of surficial materials which appear not to mask the radiation response of the bedrock. Murdama rocks give a characteristic low radiation response (figs. 26-29), particularly in the potassium and uranium channels. The contact between the Murdama and the granite body can be seen rather clearly as a steep gradient in the contours.

One potassium and thorium anomaly has been detected in the southeast corner of area 4. No apparent reason for this anomaly can be found from study of the geologic map and aerial photographs. Inasmuch as the anomaly attains only about twice the average response over the Murdama, the economic potential of the anomaly is doubtful. This anomaly should be checked if area 4 is selected for a detailed geological and geochemical investigations.

The calc-alkaline granite has a higher radiation response than the Murdama; local highs over the granite are approximately twice the average response in all three of the isoelement channels. These local highs are nearly coincident with the granite mountains rising above the pediment surface; therefore, they may be attributed to the radiation response of the mass of the mountains.

AEROMAGNETIC INTERPRETATION

During 1965-66, BRGM contracted for an aeromagnetic survey covering approximately 300,000 sq km of the Arabian Shield and including the Kùshaymiyah area. The observed total intensity data, originally compiled at a scale of 1:100,000, is shown in figure 30 at a scale of 1:250,000. The magnetic map was interpreted by Andrew Griscom (written commun. 1971) and later modified by the authors, especially in the area of the Uyaijah ring structure.

Inspection of the aeromagnetic map shows four major patterns: (1) steep gradient linear anomalies characteristic of the southwest part of the area, (2) circular and subcircular anomalies, (3) a low gradient, featureless area that occupies much of the eastern half of the map, and (4) the high intensity anomalous area bordering the eastern edge of the map. The interpretative map (fig. 31) is shown overlying a modified geologic map to compare geologic with magnetic features. Several major magnetic lineaments can be seen. The first magnetic lineament trend north-westerly and separates more magnetic rocks of the Halaban Group from the less magnetic rocks of the Murdama Group. This zone correlates well with the Najd fault.

The second major lineament trends north-northwesterly west of Jabal Al Hawshah; it is characterized by generally steep magnetic gradients. This lineament separates the more magnetic rocks of the Kushaymiyah granite complex from calc-alkaline and alkaline granite masses to the east. While it is fairly certain that the first lineament is the magnetic expression of the Najd Fault System, the second lineation may or may not be the magnetic expression of a fault contact. This contact was not recognized as a fault contact during field mapping.

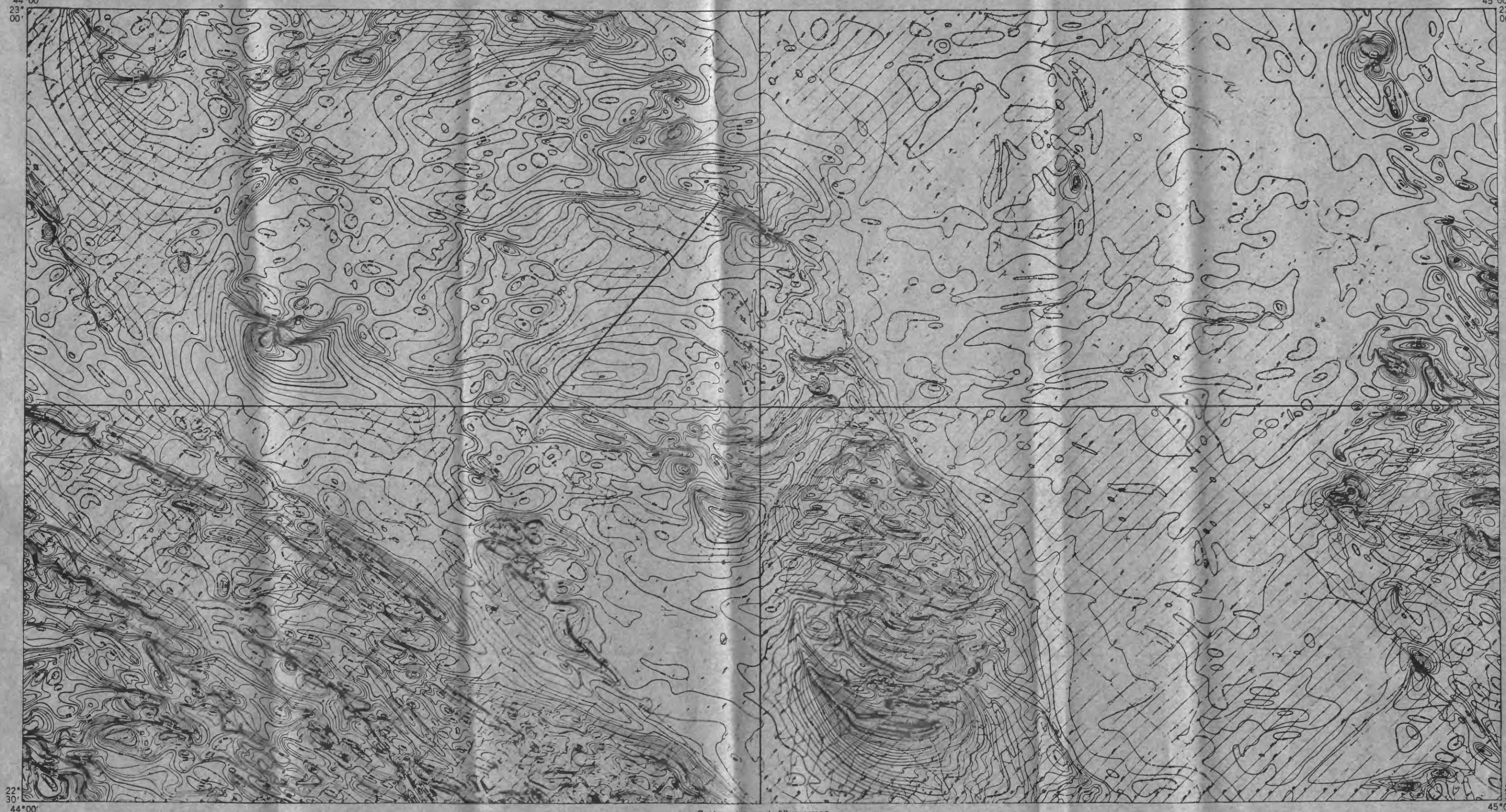

Figure 30.- Total intensity aeromagnetic map of the Kushamiyah area. A-A' is trace of observed magnetic profile.

75-657

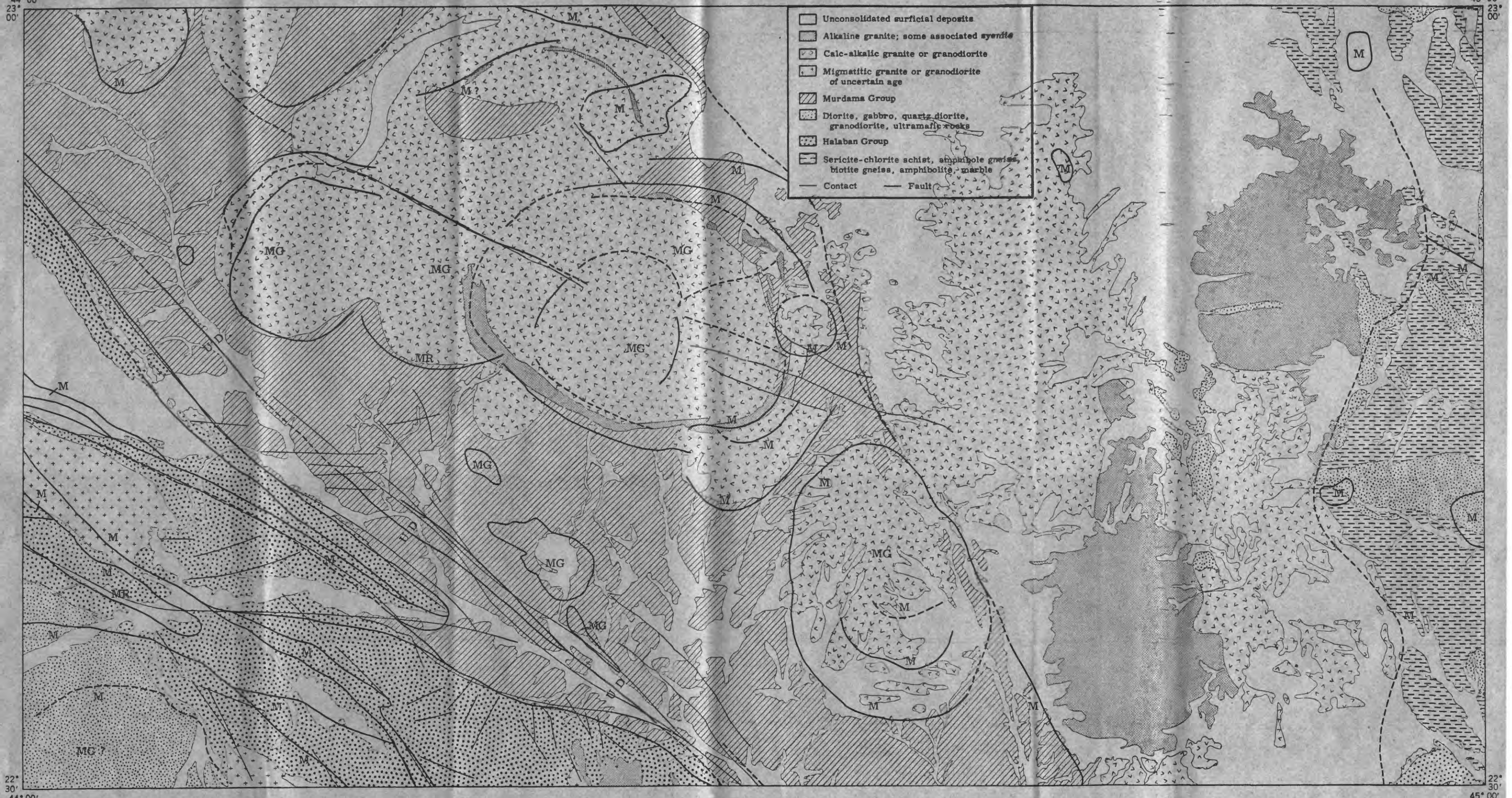

Figure 31.- Generalized geologic map of the Kushaymiyah area showing major magnetic features.

The third magnetic lineament is less well defined. It extends northwesterly from approximately the eastern edge of the Kushaymiyah granite complex nearly to the northwest corner of the map. This lineament is characterized by a series of magnetic anomalies of about 100 gamma amplitude. Some of these anomalies show the normal induced polarization pattern whereas others express an apparent remanent magnetic pattern.

The fourth is a well-defined magnetic contact between the eastern edge of the granite complexes of the Jabal Al Hawshah quadrangle and amphibole gneiss of the Ar Ridaniyah Formation. No apparent susceptibility contrast exists between the various mapped granitic rocks in the Jabal Al Hawshah quadrangle; thus, they appear magnetically as one unit characterized by a rather flat, expressionless, magnetic pattern.

The subcircular magnetic anomalies are of particular interest. Two types are apparent. The first is a filled circular anomaly characterized by a magnetic pattern which indicates the causative body is considerably more magnetic than the enclosing rocks. The Jabal Fahwah granite complex is typical of this type of magnetic expression, which is commonly seen on the Arabian Shield (Hase, 1970). The second type of circular anomaly, typified by the Kushaymiyah granite complex, is characterized by steep magnetic gradients which more or less define the outer perimeter of the body, but the interior of the body reflects about the same magnetic expression as the enclosing rocks. In the Kushaymiyah quadrangle, several bodies with this type of magnetic anomaly unite to form one complex geologic relations, circular magnetic anomalies appear to be lobes of the same body. Several smaller closed subcircular bodies are outlined by their magnetic pattern. A typical

example of the smaller plutons is a body at 22°40'N.; 44°20'E., the magnetic expression of which indicates that the near-surface size is somewhat larger than the calc-alkaline pluton mapped in this area.

Magnetically, the Uyaijah ring structure appears to have been magnetized by induction in the earth's present field. Although the anomaly is somewhat complicated, a magnetic high is present over the southern edge with a characteristic low delineating the northern edge. The gradient terminates abruptly along the east edge of the complex against a vague circular magnetic feature, with a high-amplitude anomaly delineating its south edge. The magnetic lineation paralleling the Najd Fault zone that seems to bisect the ring structure is interpreted to be a fault. However, magnetic expression of a fault ceases through the center of the ring structure, a relation here interpreted to show the fault is either deeply buried or does not exist. The magnetic character of the ring structure ranges from an essentially flat, featureless pattern in a north-south zone through the center, to low-amplitude, short wave-length anomalies in the eastern half. The rocks within the ring structure differ at least in their magnetic properties.

The ring structure is of sufficiently large dimension to permit a two-dimensional analysis. An observed magnetic profile A-A^1 (fig.32) was constructed across the ring in a direction of N.20°E. Theoretical magnetic profiles were computed and compared to the observed data. This curve-matching process assumed that the rocks were homogenous and uniformly magnetized in the direction of the earth's present magnetic field, and that the top of the body was at or near the surface. The best fit was obtained for the geometric configuration shown in figure 32.

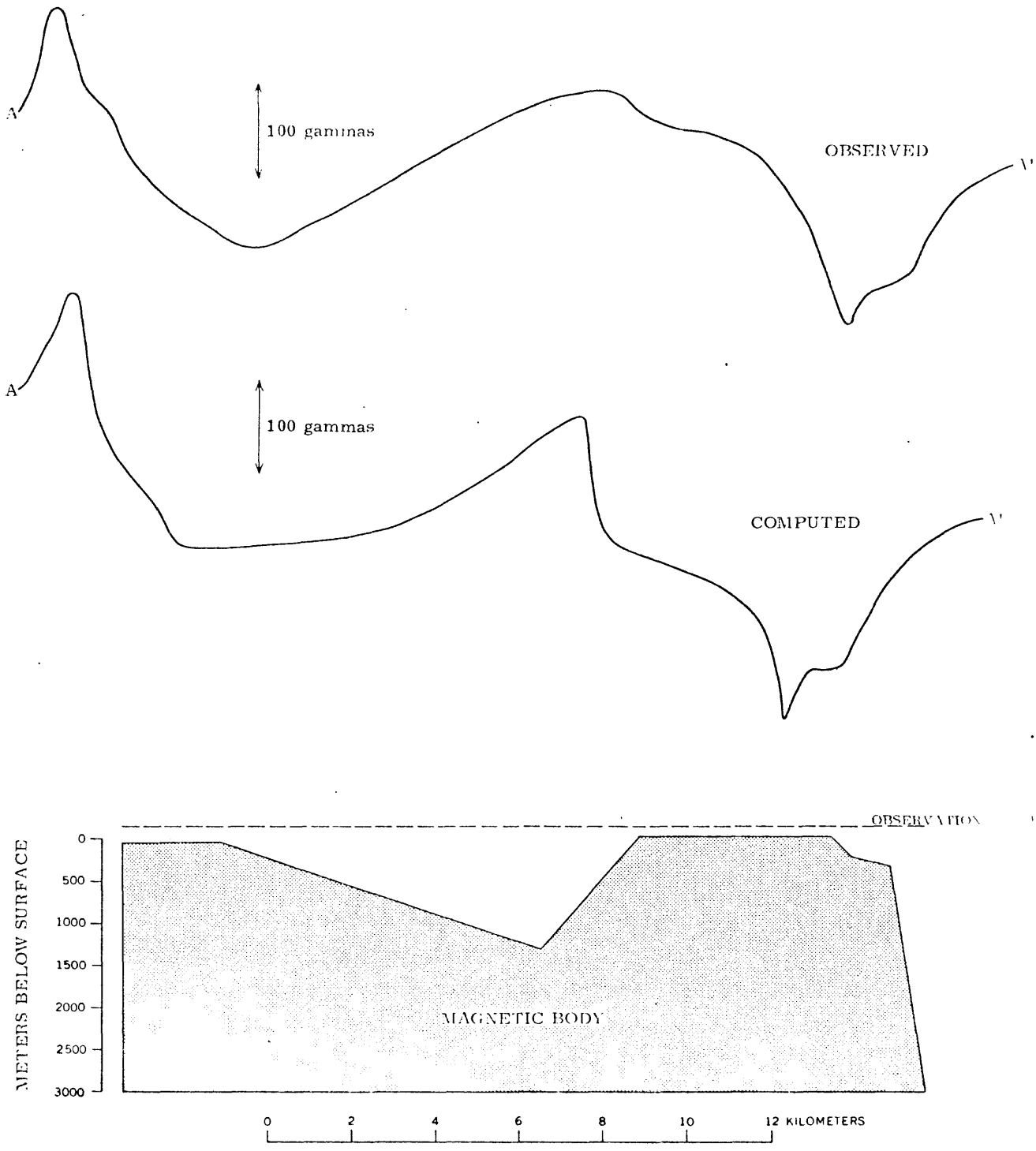

Figure 32. - Observed and theoretical total intensity magnetic profiles across the Uyaijah ring structure.

Although the model is an over-simplification, the south and north edges of the body are vertical or steeply dipping to the north. It appears that the center of the body must be nearly the shape of the model, but the right one-third of the body may be somewhat more complex than shown on the computed simple prism. It is in this area where the computed profile does not closely match the observed data. This most likely reflects the difference of magnetic properties of the granitic rocks within the ring complex. Closer control on magnetic susceptibility would assist in producing a more accurate match between computed and observed profiles.

CONCLUSIONS

The various geologic units in the area can be listed on the basis of decreasing radioactivity as follows: alkaline granite intrusives, Halaban rocks, diorite, granodiorite, and amphibole gneiss, but there is little contrast in radiation between the last four. Reasonable contacts could be inferred on the basis of radiation data between the granites and the Murdama, or between the Halaban and the Murdama, as well as between the alkaline granite and the older granite. While there is some indication that radiometric highs have been detected in areas of mineralization it will require a more detailed survey to determine the relations of the radiation response to the mimeralized areas.

Magnetic patterns which assist in understanding the regional structure and geology are: major lineations, which indicate possible faults, and/or contacts of rock units of contrasting susceptibility; circular and subcircular anomalies, both of which define magnetically unique rock units usually intrusive in nature; low-gradient, feature-less, magnetic patterns typical of granitic rocks; and high-intensity magnetic patterns typical of the intrusive phase of the Halaban.

LITERATURE CITED

Hase, D. H.; 1970, Qualitative analysis of airborne magnetometer data: The Arabian Shield, Kingdom of Saudi Arabia: U. S. Geol. Survey Saudi Arabian Project report 110, 44 p., 1 plate.

P. Lancombe, Delange, Shanti M. and Leca, X., 1970, Mineral resources and geology of the Jabal Al Hawshah quadrangle, Kingdom of Saudi Arabia: French Bur. Recherches Géol. Minières open-file rept. 70 JED 26.